AD-A115 462 NAVAL RESEARCH LAB WASHINGTON DC F/6 13/13
FLOW-INDUCED OSCILLATIONS OF OTEC MOORING AND ANCHORING CABLES:--ETC(U)
MAY 82 O M GRIFFIN
UNCLASSIFIED NRL-MR-4766 NL

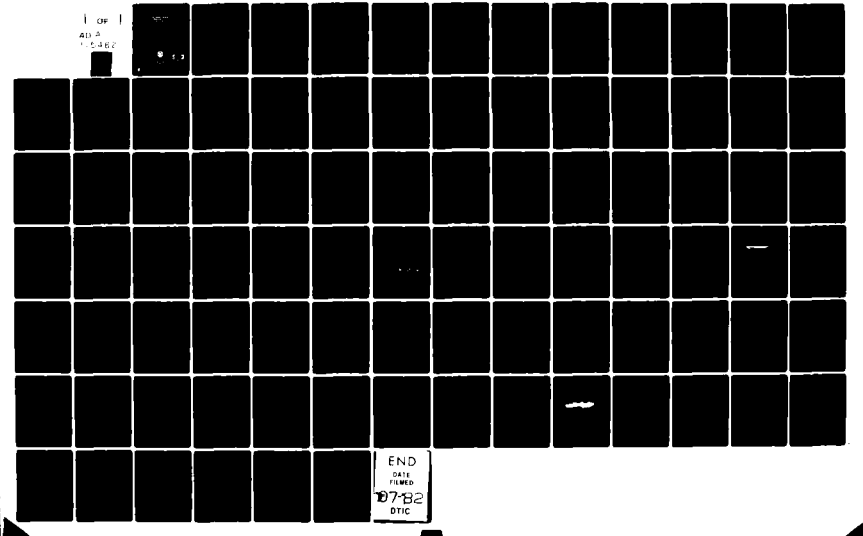

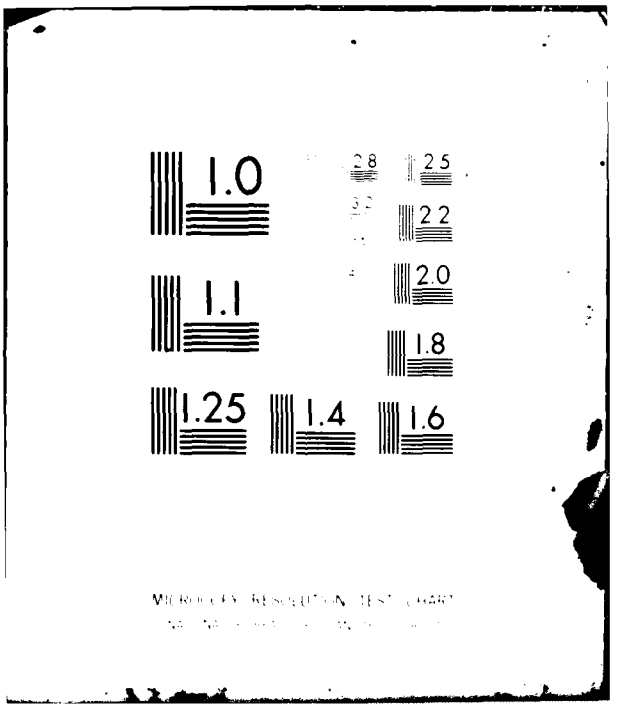
1.0
1.1
1.25
1.4
1.6
2.0
1.8
2.2
2.5

SECURITY CLASSIFICATION OF THIS PAGE (When Data Entered)

| REPORT DOCUMENTATION PAGE | | READ INSTRUCTIONS BEFORE COMPLETING FORM |
|---|---|---|
| 1. REPORT NUMBER<br>NRL Memorandum Report 4766 | 2. GOVT ACCESSION NO.<br>AD-A113 962 | 3. RECIPIENT'S CATALOG NUMBER |
| 4. TITLE (and Subtitle)<br>FLOW-INDUCED OSCILLATIONS OF OTEC MOORING AND ANCHORING CABLES: STATE OF THE ART | | 5. TYPE OF REPORT & PERIOD COVERED<br>Final<br>6. PERFORMING ORG. REPORT NUMBER |
| 7. AUTHOR(s)<br>Owen M. Griffin | | 8. CONTRACT OR GRANT NUMBER(s)<br>NOAA Project No.<br>NA 81 AAG 03089 |
| 9. PERFORMING ORGANIZATION NAME AND ADDRESS<br>Naval Research Laboratory<br>Washington, DC 20375 | | 10. PROGRAM ELEMENT, PROJECT, TASK AREA & WORK UNIT NUMBERS<br>NRL Problem 0275-C |
| 11. CONTROLLING OFFICE NAME AND ADDRESS<br>Office of Ocean Technology & Engineering Services<br>NOAA<br>Rockville, MD 20852 | | 12. REPORT DATE<br>May 27, 1982<br>13. NUMBER OF PAGES<br>87 |
| 14. MONITORING AGENCY NAME & ADDRESS(if different from Controlling Office) | | 15. SECURITY CLASS. (of this report)<br>Unclassified<br>15a. DECLASSIFICATION/DOWNGRADING SCHEDULE |

16. DISTRIBUTION STATEMENT (of this Report)

Approved for public release; distribution unlimited.

17. DISTRIBUTION STATEMENT (of the abstract entered in Block 20, if different from Report)

18. SUPPLEMENTARY NOTES

19. KEY WORDS (Continue on reverse side if necessary and identify by block number)

Ocean Engineering
Ocean Thermal Energy Conversion
Vortex Shedding
Marine Cable Strumming

20. ABSTRACT (Continue on reverse side if necessary and identify by block number)

The objective of this report is to present an overview of the state of knowledge concerned with marine cable strumming oscillations and to apply these finding of the development of design methods for deep ocean cable systems. The report emphasizes recent findings that are relevant to the design of OTEC power plant mooring and riser cable systems.

This report is limited in scope to the problems caused by vortex shedding from bluff, flexible structures and cables in steady currents, and the resulting vortex-excited oscillations. Emphasis is placed on outlining the important aspects of the basic phenomena, the development
(Continued)

DD FORM 1 JAN 73 1473 EDITION OF 1 NOV 65 IS OBSOLETE
S/N 0102-014-6601

SECURITY CLASSIFICATION OF THIS PAGE (When Data Entered)

20. ABSTRACT (Continued)

of design procedures, the definition of hydrodynamic force coefficients applicable in practice, and the specification of structural response parameters relevant to marine cable system design.

Though reasonable engineering approximations must be made, the design procedures and the experimental data base that are summarized in this and the related reports cited herein are recommended for us in cable system design practice. Procedures are described for predicting a particular system's susceptibility to vortex-excited strumming oscillations. In addition, reasonable data bases from steady and dynamic response and force coefficient measurements are provided to aid in detailed calculations of the system response, if that approach is necessary. A number of computer codes also are available to assist the designer and some have been calibrated against both field measurements and laboratory-scale test data. The analysis of the data, acquired from recent field tests, presently is underway, but additional well-controlled field tests are needed to broaden the existing data bsae.



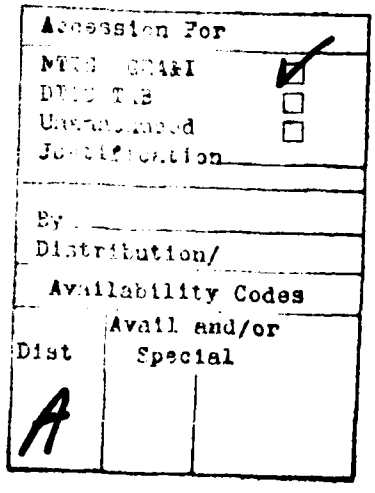

## CONTENTS

## FOREWORD AND ACKNOWLEDGMENTS

This report has been prepared by the Naval Research Laboratory as part of the OTEC ocean engineering technology development program at the Office of Ocean Technology and Engineering Services, National Oceanic and Atmospheric Administration. Funding was provided under NOAA Project No. NA 81 AAG 03089.

## NOMENCLATURE AND LIST OF SYMBOLS†

| | |
|---|---|
| $a_1$, $b_1$, $c_1$, $d_1$ | Coefficients defined in Table 5. |
| $C_{dh}$ | Unsteady force coefficient on a cylinder or cable vibrating in the cross flow direction; see equation (7). |
| $C_{mh}$ | Unsteady force coefficient on a cylinder or cable vibrating in the cross flow direction. |
| $C_D$, $C_{DO}$ | Steady drag coefficient on a vibrating (stationary) cylinder or cable. |
| $C_L$ | Lift coefficient; see equation (7). |
| $C_{LE}$ | Excitation force coefficient; see equation (7) |
| $D$ | Cable diameter (m or ft). |
| $f_n$ | Natural frequency (Hz). |
| $f_s$ | Strouhal frequency (Hz). |
| $I_i$ | Modal scaling factor; see equation (6). |
| $k_s$ | Reduced damping; see equiation (3). |
| $L$ | Cable length (m or ft). |
| $m$ | Cable physical mass per unit length (kg/m or $lb_m$/ft). |
| $m_e$ | Effective mass per unit length (kg/m or $lb_m$/ft) (physical plus added mass). |
| $m'$ | Cable virtual mass (physical plus added mass) per unit length (kg/m or $lb_m$/ft). |
| Re | Reynolds number, $VD/\nu$. |
| $Re_\nu$ | Vibration Reynolds number, $fD^2/2\nu$ |
| St | Strouhal number, $f_sD/V$. |

| | |
|---|---|
| $T$ | Cable static tension ($N$ or $lb_f$) |
| $V$ | Incident flow velocity (m/s or ft/sec or knots). |
| $V_r$ | Reduced velocity, $V/f_nD$. |
| $V_{r,crit}$ | Critical reduced velocity. |
| $w_r$ | Response parameter, $(1 + 2\ \bar{Y}/D)\ (V_r St)^{-1}$; see equation (11). |
| $\bar{x}$ | In line displacement (m or ft). |
| $\bar{X}$ | In line displacement amplitude (m or ft). |
| $\bar{y}$ | Cross flow displacement (m or ft). |
| $\bar{Y}$ | Cross flow displacement amplitude (m or ft). |
| $Y$ | Normalized displacement amplitude, $\bar{Y}/D$. |
| $Y_{EFF,MAX}$ | Normalized displacement amplitude; see equation (6). |
| $\bar{z}$ | Coordinate measurement along the cylinder or cable (m or ft). |
| $\delta$ | Log decrement of structural damping; see equation (3). |
| $\epsilon$ | Phase angle (deg or rad); see equation (7). |
| $\gamma_i$ | Normalizing factor; see equation (6). |
| $\phi$ | Phase angle (deg. or rad); see equation (7). |
| $\mu$ | Mass ratio, see equation (4). |
| $\nu$ | Kinematic fluid viscosity ($m^2$/sec or $ft^2$/sec). |
| $\rho$ | Fluid density (kg/$m^3$ or $lb_m/ft^3$). |
| $\rho_s$ | Cable density (kg/$m^3$ or $lb_m/ft^3$). |
| $\psi_i(z)$ | Mode shape for $i$th flexible beam mode; see equation (6). |
| $\zeta_s$ | Structural damping ratio; see equation (4). |

## EXECUTIVE SUMMARY

Vortex-excited oscillations of marine cable systems and structures are caused by the resonant, nonlinear interaction between the flowing water and the structure, which takes place as a result of vortex shedding. These oscillations often are characterized by a resonant wake capture or "lock-on" phenomenon in which the wake flow and the body oscillate in unison at the same frequency. At other times the vibrations are random. In the case of a cable these relatively high frequency oscillations, which are predominantly in a direction normal to the incident flow, are called *strumming*. Reduced fatigue life, large hydrodynamic forces (particularly drag) and induced stresses, increased steady and unsteady deflections, and high acoustic noise levels often accompany vortex-excited oscillations. The reliability of a cable system's performance depends on the ability to predict this dynamic behavior for conditions that are commonly found in the ocean environment.

The objective of this report is to present an overview of the state of knowledge concerned with strumming oscillations and to apply these findings to the development of design methods for cable systems that are likely to undergo these oscillations. The report emphasizes recent findings that are relevant to the design of OTEC power plant mooring and riser cable systems.

This report is limited in scope to the problems caused by vortex shedding from bluff, flexible structures and cables in steady currents, and the resulting vortex-excited oscillations. Emphasis is placed on outlining the important aspects of the basic phenomena, the development of design procedures, the definition of hydrodynamic force coefficients applicable in practice, and the specification of structural response parameters relevant to marine cable system design.

Section 3 of this report gives an overview of the present state-of-the-art concerning the vortex-excited oscillations of flexible, cylindrical structures with nominally circular cross-sections. Particular attention is given to the behavior of a cable in a flowing fluid and to the specification of the steady and

unsteady hydrodynamic forces and the resonant vibration response characteristics. Other factors such as surface roughness, nonuniform (shear) flow effects and yaw or inclination of the cable to the flow are discussed briefly.

Also in Section 3 of the report a discussion is given of recent experimental studies of cable strumming. The physical scales of the experiments range from relatively small flow channels, to large towing channels and to field experiments in the oceanic environment. The field experiments encompass relatively small-scale tests conducted in a tidal inlet and large-scale, deep water tests of moored arrays.

Analytical models which have been developed for the prediction of cable strumming are discussed in Section 4 of the report. The various modelling approaches taken by different investigators are reviewed, and recommendations are made for applications to the cable design process. Comparisons are made between the model predictions and available experimental data from both laboratory and field scale tests. A discussion is given of the prediction methods and design procedures which have been developed and calibrated for practical applications.

Computer codes for predicting and modelling cable strumming are described in Section 5. The codes that have been developed for ocean engineering applications comprise two areas of application: the static analysis of cable arrays and the dynamics of marine cables. NATFREQ is a code for calculating natural frequencies, mode shapes, and drag amplification factors for taut cables with attached masses. DESADE and DECEL 1 are two versions of a code that was developed to statically analyze structural marine cable arrays. This code includes a resonant vibration analysis routine which calculates the static deflections of the array due to the added drag forces that accompany strumming oscillations. SEADYN is a nonlinear finite element cable system model being developed by CEL. A wide variety of systems can be modeled, including: pay-out and reel-in, time varying current fields, and point loads. The Skop-Griffin strumming model has been incorporated into SEADYN. SLAK is a finite-element computer code that was originally developed for the analysis of the free vibrations of slack cables in three dimensions. This code has been adapted at NRL for ocean engineering calculations of cable

equilibrium shapes, support reaction forces, natural frequencies and the mode shapes with respect to the equilibrium position. Several additional codes which may be applicable to cable strumming analyses also are discussed briefly.

Section 6 of the report presents a brief discussion of cable strumming suppression devices and procedures. Examples are given of typical devices which have been used successfully to suppress the strumming oscillations of marine cables caused by vortex shedding.

The final section of the report is a brief discussion of marine cable strumming problems in terms of OTEC cable problems.

# FLOW-INDUCED OSCILLATIONS OF OTEC MOORING AND ANCHORING CABLES: STATE OF THE ART

## 1. INTRODUCTION

*1.1 Objectives.* The permanent offshore mooring of large ocean thermal energy conversion (OTEC) power plants in 1200 m (3900 ft) to 1800 m (5900 ft) water depths is an engineering undertaking that requires an exacting and well-organized development program. To this end an OTEC mooring system technology development plan (1) has been formulated to accomplish this task.

According to this plan the mooring system must be designed for 10-year operation of the pilot plant and for 30-year operation of a commercial OTEC plant. The replacement cycle of mooring system components due to the effects of corrosion, abrasion and fatigue is at present an important, but unanswered, question in relation to the mooring system design and economy of construction. The OTEC mooring system must be reliable enough to be insurable, safe enough to be workable, and simple enough and unobstructive enough to allow easy access for repairs and replacement.

One aspect of the mooring system dynamics is the small-displacement, "high frequency" response generated by vortex shedding as water flows past the mooring cables. This response is commonly referred to as cable strumming. The objective of this report is to describe the state-of-the-art for predicting the dynamic strumming response of marine cable systems, insofar as this dynamic fluid/structure interaction is relevant to the design of the OTEC mooring cable system. The results from this report also are applicable in general to the OTEC riser power cable.

*1.2 Background.* It is often found that bluff, or unstreamlined, structures display some form of undesirable oscillatory instability arising from motion relative to a surrounding fluid. A common

Manuscript submitted January 5, 1982.

mechanism for resonant, flow-excited oscillations is the organized and periodic shedding of vortices as the flow separates alternately from opposite sides of a long, bluff body. The flow field exhibits a dominant periodicity and the body is acted upon by time-varying pressure loads. These result in steady and unsteady drag forces in line with the flow and unsteady lift or side forces perpendicular to the flow direction. If the structure is flexible and lightly damped internally as in the case of a cable, then resonant oscillations can be excited normal or parallel to the incident flow direction. For the more common cross flow oscillations, the body and the wake have the same frequency of oscillation which is near one of the characteristic frequencies of the structure. The shedding meanwhile is shifted away from the natural, or Strouhal, frequency at which pairs of vortices would be shed if the structure were restrained from oscillating. This phenomenon is known as "lock-on" or "wake capture."

The vortex-excited oscillations of marine cables, commonly termed *strumming*, result in early fatigue, increased steady and unsteady hydrodynamic forces, and amplified acoustic flow noise. They sometimes lead to structural damage and possibly to failure. Flow-excited oscillations very often are a critical factor in the design of underwater cable arrays, mooring systems, riser systems, and offshore platforms such as an OTEC power plant, since these complex structures usually have bluff cylindrical shapes which are conducive to vortex shedding when they are placed in a flow. An understanding of the basic nature of the fluid/structure interaction which produces vortex-excited oscillations is an important consideration in the reliable design of offshore structures and cable systems.

Problems associated with the shedding of vortices often have been neglected in the past in relation to the design of offshore platforms and cable structures, largely because reliable experimental data and design methods have not been available. However, the dynamic analysis of ocean structures and cable systems has become an important consideration in the prediction of stress distributions and fatigue life in the offshore environment. These factors are particularly relevant as new and more complex systems must be designed to withstand the deep ocean environment over long time periods. Reliable experimental data are now in hand for the dynamic response of and flow-induced forces on a

model scale. Based upon these experiments, semi-empirical prediction models have been developed and favorably compared with field test data.

*1.3 Scope of the Report.* This report is limited in scope to the problems caused by vortex shedding from marine cable structures and moorings, and to the resonant cross flow or strumming oscillations that often are excited by the vortices. The topics discussed in this report are primarily relevant to problems associated with the mooring and riser cables for OTEC power plants. A discussion is given of the basic fluid dynamic characteristics of a cable in an incident flow, including the steady and unsteady hydrodynamic forces, resonant dynamic response characteristics, and the static response caused by amplified hydrodynamic drag forces. Relevant experimental findings from towing channel experiments, small-scale field experiments and large-scale field experiments also are discussed.

Strumming analysis methods for both taut and slack marine cables are described together with the computer codes that are available to implement the various analysis procedures. Emphasis is placed here on the development of design procedures, on the definition of hydrodynamic loads and force coefficients applicable in practice, and on the definition of structural and hydrodynamic response parameters relevant to marine cable design. All of these topics are discussed in more detail in a related report (2).

## 2. BASIC CHARACTER OF VORTEX SHEDDING.

The frequency $f_s$ of the vortex shedding from a circular cylinder is related to the other main flow parameters ($D$, the diameter of the cylinder; $V$, the flow velocity) through the nondimensional Strouhal number defined as

$$St = \frac{f_s D}{V}.$$

The value of the Strouhal number varies somewhat in different regimes of the Reynolds number and with the shape of the cylinder (circular, $D$-section, triangular, etc). For the range of the Reynolds number where the Strouhal number remains constant the relation between the shedding frequency and the velocity is linear for a given cylinder, i.e.

$$f_s = KV,$$

where $K = St/D$. If a cylinder immersed in a flowing fluid is free to oscillate in the cross-flow direction, then the latter relation does not hold in the vicinity of the natural frequency of the cylinder. This resonance phenomenon—called "lock-on" or wake capture—is discussed in this paper.

If the Reynolds number is lower than about $10^5$, then the vortex shedding is predominately periodic and the value of the Strouhal number can be roughly assumed to be 0.2 for a circular cylinder or cable. Measurements of the frequencies, displacement amplitudes and forces which result from vortex-excited oscillations have been obtained by many investigators from experiments both in air and in water. Some of the most recent of these experiments and related studies are summarized here in order to provide background for the OTEC cable problems. A detailed but somewhat selective review of the basic aspects of the problem of vortex-excited oscillations in general has been made recently by Sarpkaya (3). King (4) and Griffin (5,6) have discussed the subject in the context of ocean engineering applications.

## 3. EXPERIMENTAL CABLE STRUMMING RESULTS

### 3.1 Basic Character of Cable Strumming.

*3.1.1 Resonant response characteristics.* A typical structure used for experimental vortex shedding studies consists of a cylinder positioned perpendicularly to the flow and flexibly supported at each end. Representative measurements for such a cylinder in air have been reported by Griffin and Koopmann (7) and in water by Dean, Milligan and Wootton (8). The results obtained are generally the same in both media. As the incident flow velocity $V$, or the "reduced velocity" $V_r$ as in Figure 1, is increased the unsteady displacement amplitude first builds up to a maximum, after which it begins to decrease as the upper limit of the resonance is approached. For one example shown in the figure the lock-on range, defined by vibration displacements greater than the resonant threshold ($2\bar{Y}/D = 0.1$), is given by reduced velocities between $V_r = 4.5$ and 7.5 in air, with the maximum of $\bar{Y}/D$ occurring at $V_r \sim 6$. For the in-water experiments the resonance range is somewhat wider, from $V_r = 4$ to nearly 8, but the peak value of $\bar{Y}/D$ again is excited at $V_r \sim 6$.

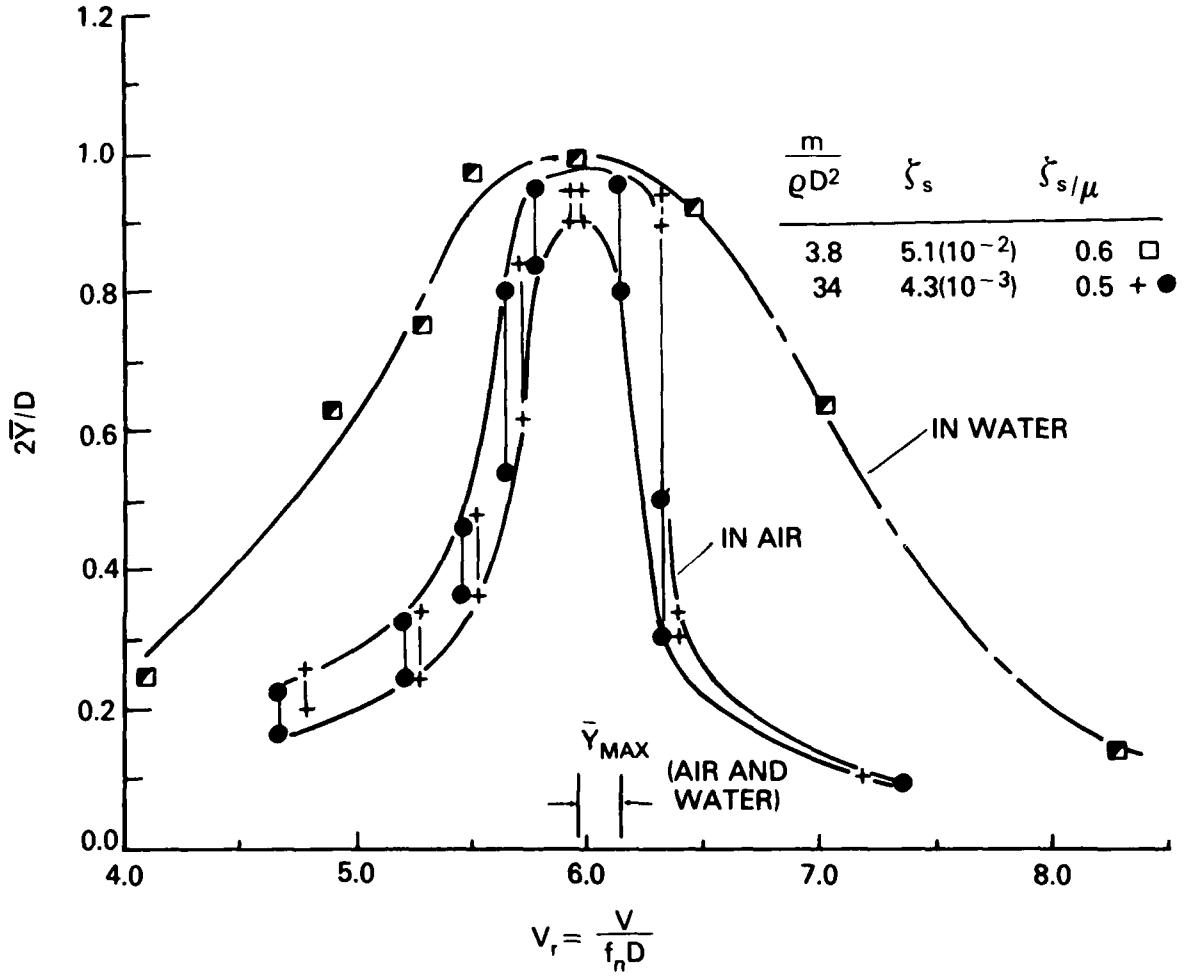


Fig. 1 — The cross flow displacement amplitude $2\bar{Y}/D$ for a circular cylinder plotted against the reduced velocity $V_r = V/f_n D$

The narrow resonance band in air is typical of lightly-damped systems while the more broad resonance in water is typical of systems with relatively higher structural damping. It can be seen that even though the damping and mass ratios of the two systems differ by factors of ten, the *reduced damping* (the product of the mass ratio and the structural damping ratio, equation (3) or (4)) is very nearly the same and so are the peak displacement amplitudes for the two cylinders. This overall pattern of behavior is typical of measurements in water and similar fluids at all Reynolds numbers where vortex shedding takes place.

The cross-flow response of an isolated model pipe to steady currents is shown in Figure 2. The characteristic response is similar to those in Figure 1, but there also are some important differences. A hysteresis-like effect in the response of the model pipe was observed by Tsahalis and Jones (9) in their experiments, and they attribute this finding to nonlinearities in the elastic system. Essentially, a different dependence of the displacement amplitude upon the reduced velocity is present depending upon whether the current speed is increasing from low values or is decreasing from high values. A similar explanation for hysteresis effects in the aeroelastic response of circular cylinders was put forward some years ago by Currie, Hartlen and Martin (10). Despite the differences between the results in Figures 1 and 2, it is safe to say that a flexible cylinder in water will undergo large-amplitude cross flow oscillations whether or not the elastic system is linear or nonlinear. However, the results obtained by Tsahalis and Jones and shown in Figure 2 underscore the importance of giving careful consideration to the elastic structural system in the overall hydroelastic design of a marine system such as a pipeline, a riser, or a cable array.

The objective of the experimental program conducted by Tsahalis and Jones was to study the effects of wall proximity on vortex shedding from flexible circular cylinders in steady currents. Problems caused by boundary proximity are important considerations in the design and operation of marine pipelines near the ocean floor. The effects of wall proximity are not considered further in this report because of the relative unimportance of such effects to cable design, but additional discussion of vortex shedding from cylinders near plane boundaries is given by Buresti and Lanciotti (11).

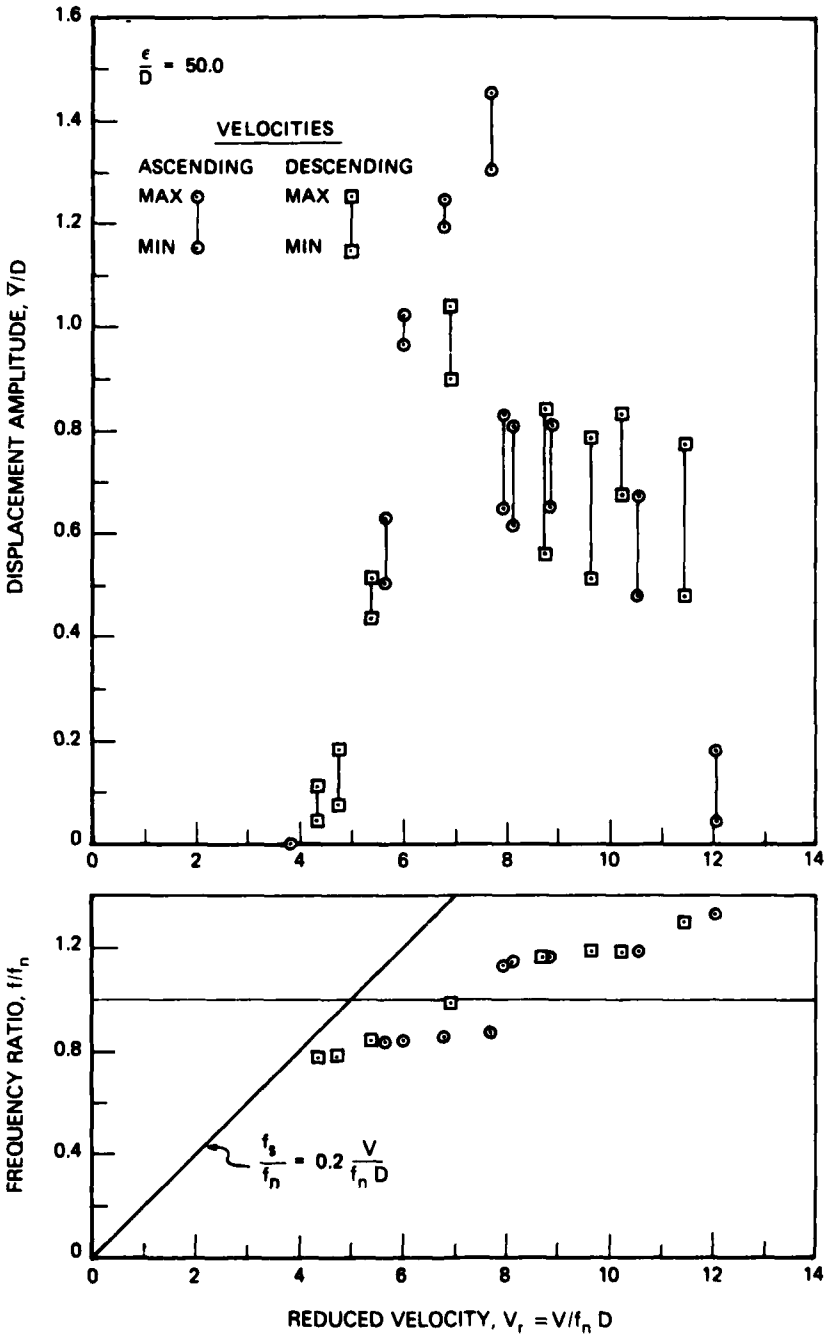


Fig. 2 — The cross flow displacement amplitude and frequency responses of a flexible model pipe due to vortex shedding; from Tsahalis and Jones (9). The isolated model (gap-to-wall ratio = 50) had a length-to-diameter ratio $L/D$ = 150 and a specific gravity of 2.4. The original figure was provided by the Shell Development Company.

When Reynolds and Froude number effects are not important, the peak vortex-excited displacement amplitude in the cross flow direction can be expressed from dimensional analysis as being dependent on three quantities (4, 12, 13), namely,

$$\bar{Y}_{MAX} = f\left(\frac{f_s}{f_n}, \zeta_s, \mu\right). \tag{1}$$

Here $f_s/f_n$ is the ratio of the Strouhal and structural frequencies $f_s = St\ V/D$ and $f_n$, respectively; and $\zeta_s$ is the structural damping ratio. The parameter $\mu$ is a mass ratio, defined by $\mu = \rho\ D^2/8\pi^2 St^2 m$, which also results from the normalization of the force coefficients in the governing equations of structure or cable motion as shown by Griffin and Koopmann (7) and Sarpkaya (3,14), for example. When there is a scale effect or a dependence upon Reynolds number, say between a laboratory model and a full-scale prototype, the "size number" or the product of the Strouhal and Reynolds numbers should be modeled as closely as possible. This parameter is given by

$$St\ Re = \frac{f_n D^2}{\nu}. \tag{2}$$

Previously it was noted that the peak in line displacement amplitude is a function primarily of a response or reduced damping parameter of the form

$$k_s = \frac{2m\delta}{\rho D^2}. \tag{3}$$

This formulation of the reduced damping can be written in the analogous form

$$\zeta_s/\mu = 2\pi\ St^2 k_s \tag{4}$$

when the damping is small and $\zeta_s = \delta/2\pi$. The importance of the reduced damping follows directly from resonant force and energy balances on the vibrating structure, as shown by Griffin (15) and Sarpkaya (3,14). Moreover, the relation between $Y_{MAX}$ and $k_s$ or $\zeta_s/\mu$ holds equally well for flexible cylindrical members such as cables with normal mode shapes given by $\psi_i(z)$, for the $i$ th mode.

If the cross flow displacement (from equilibrium) of a flexible structure with normal modes $\psi_i(z)$ is written as

$$y_i = Y\psi_i(z) \sin \omega t \tag{5}$$

at each spanwise location $z$, then the peak displacement is scaled by the factor (16,17)

$$Y_{EFF,MAX} = YI_i^{1/2}/|\psi_i(z)|_{MAX} = Y/\gamma_i, \quad Y = \bar{Y}/D, \tag{6a}$$

where

$$I_i = \frac{\int_0^L \psi_i^4(z)\,dz}{\int_0^L \psi_i(z)\,dz}, \tag{6b}$$

and

$$\gamma_i = \frac{|\psi i(z)|_{MAX}}{I_i^{1/2}}. \tag{6c}$$

The effective value $Y_{EFF}$ is derived from considerations based on several versions of the so-called "wake oscillator" formulation for modelling vortex-excited oscillations (16,17).

Experimental data for $Y_{EFF}$ as a function of $\zeta_s/\mu$ are plotted in Figure 3. These results encompass a wide range of single cylinders of various configurations and flexure conditions at Reynolds numbers from 300 to $10^6$. The various types of structures represented by the data points are given in Table 1. As a typical example, King (18,19) measured the deflections of a flexible cantilever in the fundamental mode. Peak-to-peak displacements as great as 2 to 4 diameters were measured for length/diameter ratios up to 50 (19) and 240 (8). All available experiments to date indicate that the limiting unsteady displacement amplitude for a flexible circular cylinder is about $2Y_{EFF} = 2$ to 3 at low values of reduced damping.

These results have been obtained both in air and in water, even though the mass ratios of vibrating structures on the two media differ by two orders of magnitude. For typical structures vibrating in water the mass ratio $\frac{2m}{\rho D^2}$ varies from slightly greater than 2 to about 10; in air the mass ratios corresponding to Figure 3 typically vary from $\frac{2m}{\rho D^2} = 30$ to 1000.

*3.1.2 Unsteady hydrodynamic loads.* When a cylindrical body resonantly vibrates due to vortex shedding, the periodic motion is accompanied by increased coherence of the vortex shedding lengthwise along the body and by an amplification of the unsteady fluid forces. Though a number of measurements of the forces have been made, only recently has attention been given to understanding the

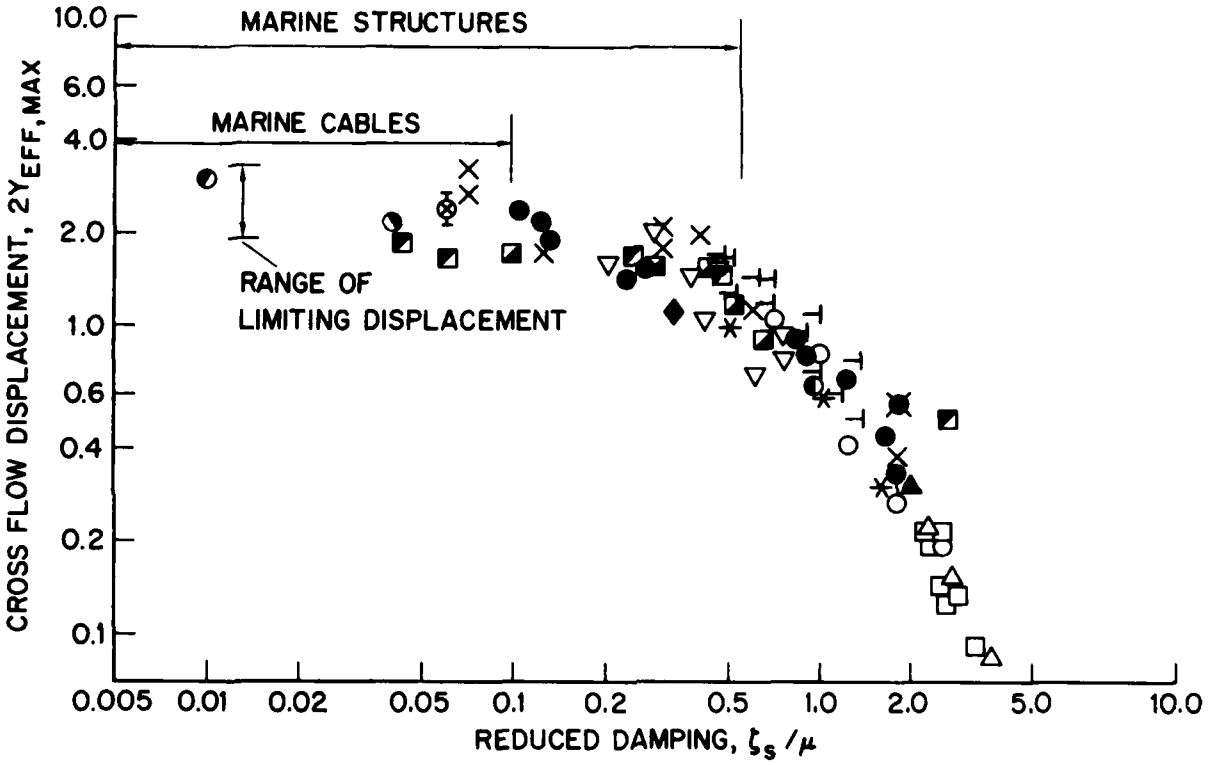


Fig. 3 — Maximum vortex-excited cross flow displacement $2Y_{EFF,MAX}$ of circular cylinders, scaled as in equation (6), as a function of the reduced damping $\zeta_s/\mu = 2\pi S^2 k_s$

Table 1
Vortex-excited Cross Flow Displacement Amplitude Response of Cylindrical Structures.
Legend for Data Points in Fig. 3

| Type of cross-section and mounting; medium | Symbol |
|---|---|
| Various investigators, from Griffin (15): | |
| Spring-mounted rigid cylinder; air | *○⊣▣◐ |
| Spring-mounted rigid cylinder; water | ◆ |
| Cantilevered flexible circular cylinder; air | Δ |
| Cantilevered flexible circular cylinder; water | X▽⊕ |
| Pivoted rigid circular rod; air | □▲ |
| Pivoted rigid circular rod; water | ● |
| From Dean, Milligan and Wootton (8): | |
| Spring-mounted rigid cylinder; water | ◩ |
| Flexible circular cylinder, $L/D$ = 240; water | ◪ |
| From King (19): | |
| Cantilevered flexible circular cylinder, $L/D$ = 52 (PVC); water | ◴ |
| Cantilevered flexible circular cylinder, $L/D$ = 52 (stainless steel); water | ◕ |

mechanisms by which this fluid-structural interaction force is generated (3,15) and how results may be scaled with confidence to large Reynolds numbers (20).

The fluid forces which act on a resonantly vibrating, cylindrical structure due to vortex shedding have been characterized recently (15,21) and the various components of the total hydrodynamic force are:

- The exciting force component, by which energy is transferred to the structure;
- The reaction, or damping force, which is exactly out-of-phase with the structures velocity;
- The "added mass" force, which is exactly out-of-phase with the structure's acceleration;

and

- The flow-induced inertial force.

The various components can be deduced from the total hydrodynamic force as measured, say, by Sarpkaya (3,14) or the various components can be measured individually as shown by Griffin and Koopmann (7). This point is discussed at greater length in references 2 and 5.

Some typical forced cylinder measurements reported by Sarpkaya appear in Figures 4 and 5. The measured values for the inertia coefficient $C_{mh}$ shown in Figure 4 as a function of the reduced velocity $V_r$, for a displacement from equilibrium of $Y/D = 0.5$. Of particular note is the marked variation in $C_{mh}$ in the vicinity of $V_r = 5$. This effort corresponds to the large phase shift in the fluid force relative to the vibratory displacement when the characteristic frequency of the flow is locked onto the vibration frequency. The fluid force on the cylinder is dominated at low reduced velocities by inertia contributions at the cylinder frequency.

The drag or resistance force $C_{dh}$ is plotted in Figure 5 as a function of $V_r$ at the same displacement. This component of the total fluid dynamic force is negative and becomes dominant near $V_r = 5$. In effect, $C_{dh}$ is the *negative of the lift coefficient* as it is usually characterized, so that the negative value of $C_{dh}$ near $V_r = 5$ suggests a net transfer of energy from the flow to the cylinder in that region. These forced-cylinder results are comparable to the vortex-excited forces which act upon resonantly vibrating cylinders when the reduced damping is sufficiently small as in the left-hand portion of Figure 3.

The excitation component of the total unsteady hydrodynamic force is defined as

$$C_{LE} = C_L \sin \phi = -C_{dh} \cos \epsilon \tag{7}$$

and is important because it is this component of the total force that transfers energy to the vibrating structure. Here $\epsilon$ and $\phi$ are phase angles between the hydrodynamic force and the motion of the structure (15). The maximum value of the force coefficient $-C_{dh}$ in Figure 9 occurs near $V_r = 5$, and similar results were obtained at the displacements $\overline{Y}/D = 0.13$, 0.25, and 0.75. A number of measurements of $C_{LE}$ by various means are plotted against the effective displacement amplitude in Figure 6 and Table 2 describes the various conditions under which the experimental results were obtained. Several

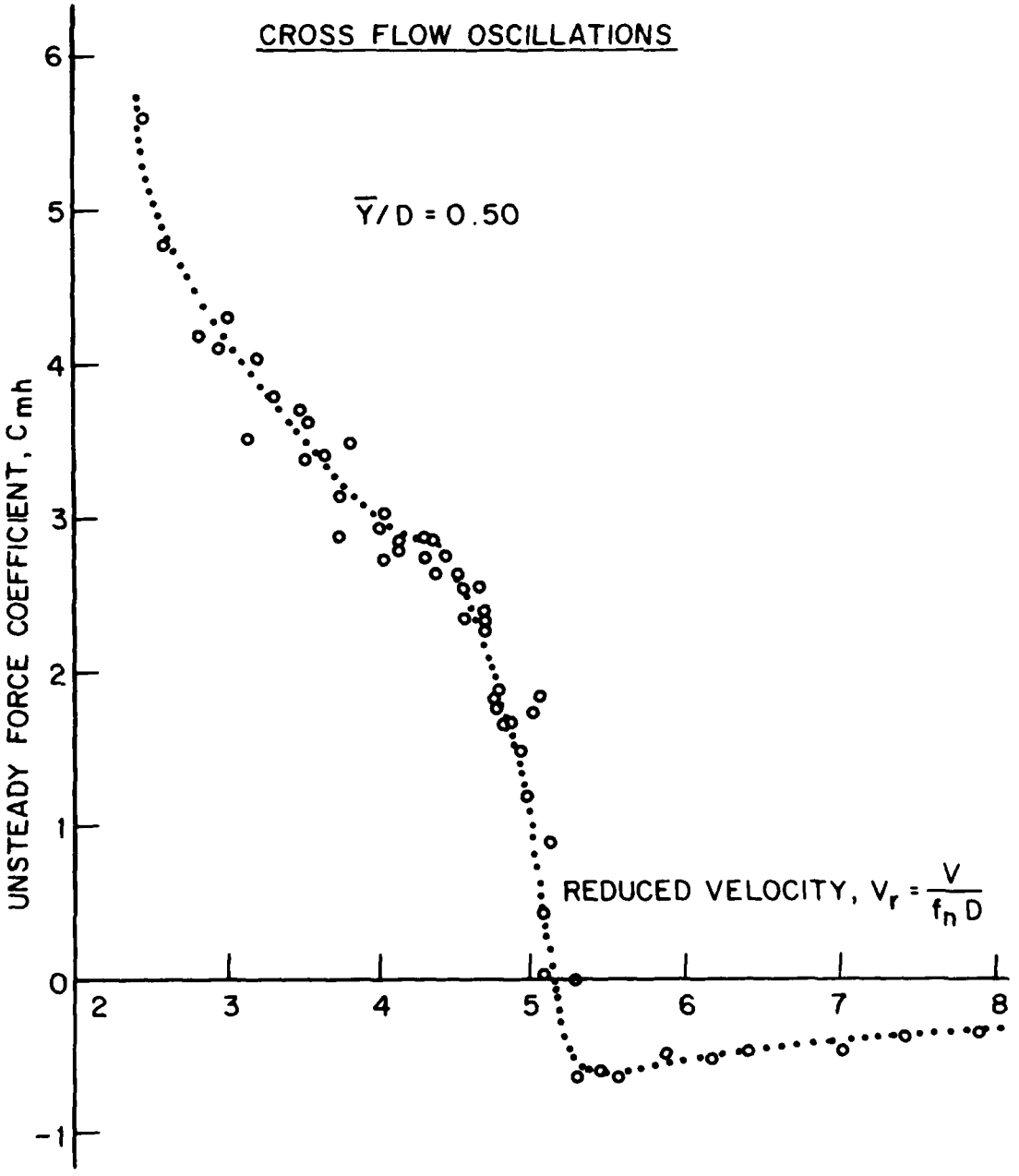


Fig. 4 — The inertia coefficient $C_{mh}$ at the vibration frequency plotted against the reduced velocity $V_r$ for $\bar{Y}/D = 0.5$; from Sarpkaya (14)

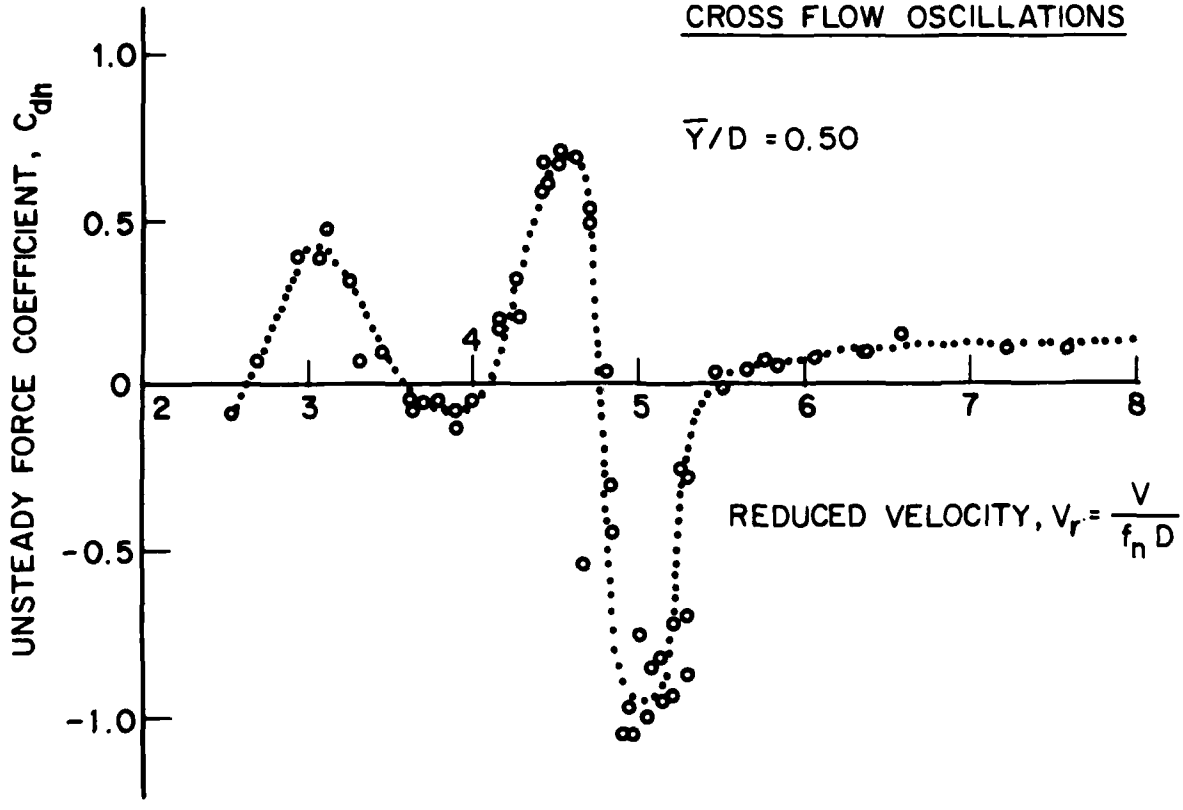


Fig. 5 — The "drag" coefficient $C_{dh}$ at the vibration frequency plotted against the reduced velocity $V_r$ for $\bar{Y}/D = 0.5$; from Sarpkaya (14)

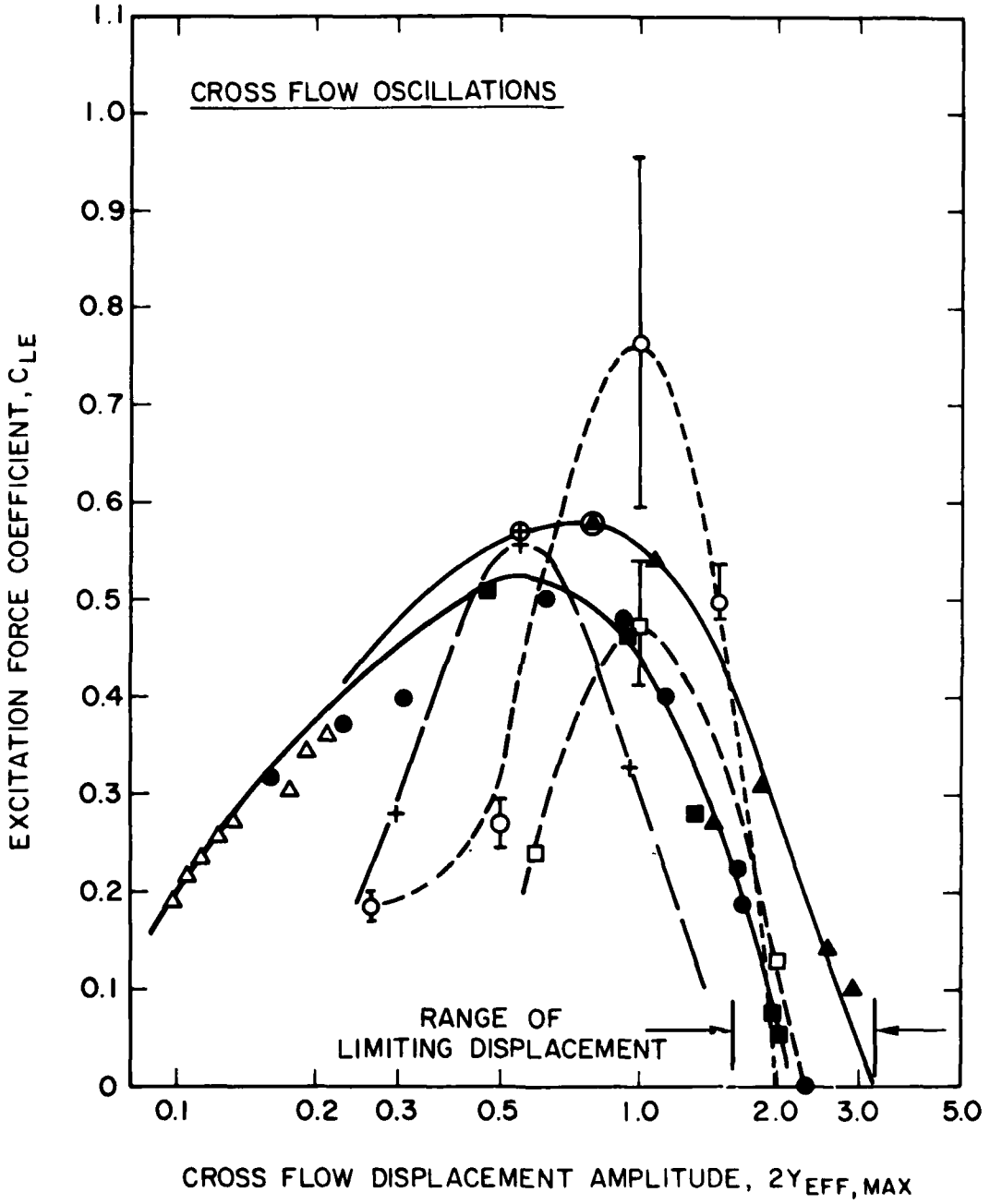


Fig. 6 – The excitation component $C_{LE}$ of the lift force plotted against the vortex-excited flow displacement $2Y_{EFF,MAX}$ (peak-to-peak), as in Eq. (7). The legend for the data points is given in Table 2.

Table 2
The Excitation Force Coefficients on Vibrating Bluff Cylinders; Description of the Data in Fig. 6

| Symbol | Type of cylinder | Medium | Cylinder material | Investigator(s) |
|---|---|---|---|---|
| ▲ | Flexible cantilever | Water | PVC | King (1977) |
| ■ | | | PVC<br>Aluminum<br>Stainless steel | |
| ● | Pivoted rigid cylinder | Water & Air | Brass | Vickery and Watkins (1964) |
| + | Spring-mounted rigid cylinder | Air | Aluminum tubing | Griffin and Koopmann (1977) |
| □ | Rigid cylinder, forced oscillations | Water | Stainless steel | Mercier (1973) |
| ○ | Rigid cylinder, forced oscillations | Water | Aluminum tubing | Sarpkaya (1978) |
| Δ | Flexible cantilever | Air | Aluminum | Hartlen, Baines and Currie (1968) |

important characteristics of the unsteady lift and pressure forces that accompany vortex-excited oscillations are clear from the results. First there is a maximum of the excitation force coefficient at a peak-to-peak displacement between 0.6 and 1 diameters for all the cases shown in the figure. Second, the maximum of the force coefficient is approximately $C_{LE} = 0.5$ to 0.6 for all but one case, the sole exception being the result at $C_{LE} = 0.75$. $C_{LE}$ then decreases toward zero in all cases and results in a limiting effective displacement of 2 to 3 diameters (peak-to-peak). This limiting amplitude is clearly shown at low values of reduced damping in Figure 3.

The coefficient $C_{LE}$ represents only the excitation component of the total unsteady hydrodynamic force. It also is necessary to have accurate and precise values for the other force coefficients such as the added mass, damping, and inertia effects described above. A complete discussion of these forces is given by Griffin (5,15).

*3.1.3 Steady hydrodynamic drag forces.* An important effect which accompanies the resonant cross flow oscillations of structures and cables due to vortex shedding is an amplification of the steady drag force (or the drag coefficient $C_D$). The drag amplification under a variety of conditions has been measured and the results have been reported by Griffin and Ramberg (22). A methodology for employing these measurements in the analysis of marine cable structures was developed by Skop, Griffin and Ramberg (23). This procedure has been generalized to the case of flexible, cylindrical marine structures by Griffin (5,6) in a study of the OTEC cold water pipe's vulnerability to flow-induced oscillations. A step-by-step approach to this problem is discussed in a later section of this report.

Measurements of the vortex-excited cross flow oscillations of model marine piles were made by Fischer, Jones and King (19,24) as part of a study of pile installation procedures during construction of the Cognac platform in the Gulf of Mexico. The steady deflection at the free end of the model pile also was measured; in this case the model was a simple, uniform cantilever beam with no tip masses, fully immersed in water, and normal to the incident flow. For low flow velocities the measured and predicted tip deflections coincided when the pile was effectively stationary. The deflection was predicted by assuming a uniform loading

$$w(x) = 1/2\ \rho V^2 D C_D(x)$$

over the length of the flexible beam in which the constant drag coefficient $C_D(x)$ was a constant, $C_D = 1.2$.

When the critical flow velocity for the onset of the vortex-excited oscillations was exceeded, the measured steady deflections in line with the flow departed significantly from the predicted reference curve. The results are plotted in Figure 7. For the lower values of relative density the flow velocities above the threshold value caused steady deflections of up to twice the value predicted by assuming $C_D = 1.2$. For the higher values of relative density, the steady deflections of the model diverged from the predicted curve, reached a maximum, and then returned to the predicted curve as the flow velocity was increased still further. The region of divergence corresponds directly to the range of resonant, large amplitude cross flow oscillations that also were measured by Fischer, Jones, and King (19,24).

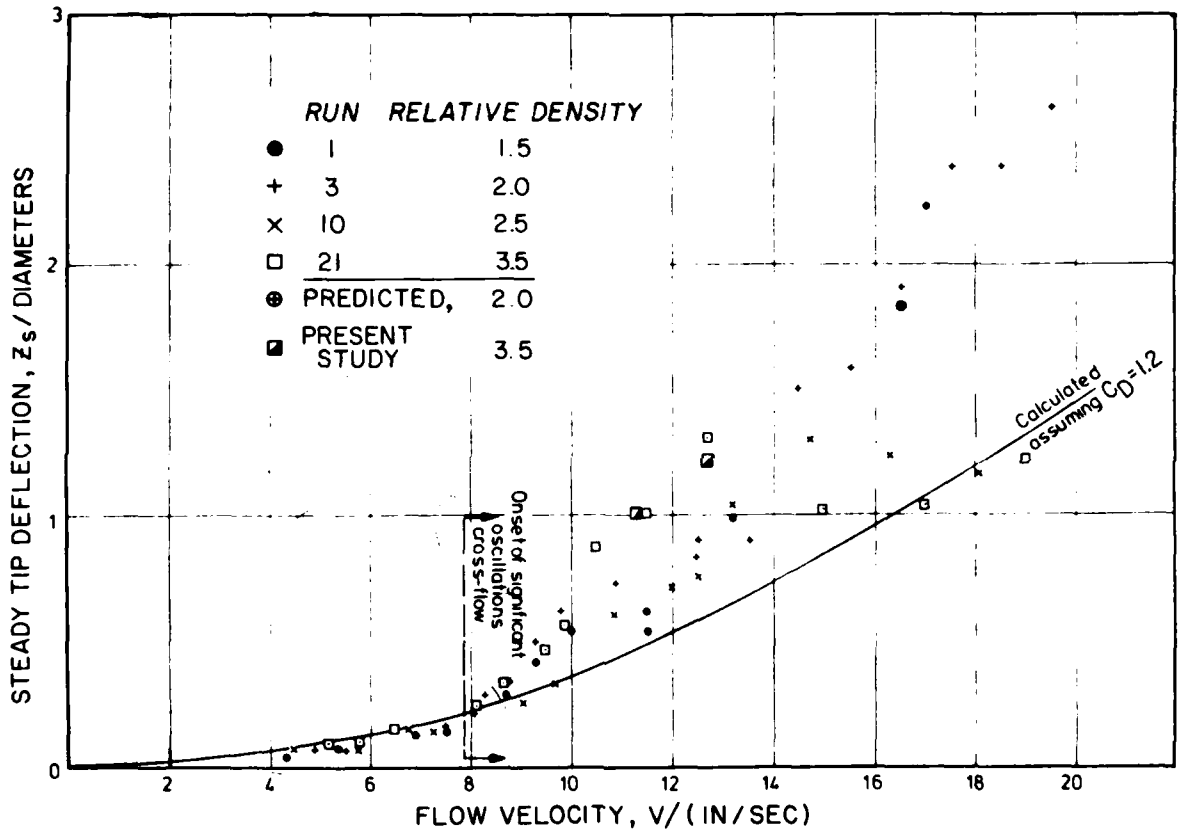


Fig. 7 — Drag-induced steady deflection at the tip of a free-ended cantilever marine pile. The pile was oscillating perpendicular to the incident flow in the resonant response regime shown for water velocities greater than $V$ = 8 in/sec; from King (19). The calculated points are from Griffin (6).

For example, the tip of the $SG = 3.5$ pile was deflected in line about 1.3 diameters at a water velocity $V$ of 13 in/sec (0.64 kt). At this same flow velocity the cross flow displacement amplitude was $\pm 1.5$ diameters. If the pile was restrained from oscillating, then the steady deflection of the tip was predicted to be 0.6 diameters at the same flow velocity.

A program of tests, conducted at the David Taylor Naval Ship R&D Center during the 1940's and released a few years ago, demonstrated the strong resonance due to vortex shedding that took place when a bare circular cylinder was towed through water and underwent large-amplitude cross flow oscillations (25). This cylinder was later fitted with various vortex suppression devices in order to investigate their effectiveness in suppressing the cross flow oscillations. The drag on the cylinder was measured over a range of towing speeds up to 10 knots and the results are plotted in Figure 8. A clear resonance occurred near $V = 4$ knots and the drag force (and coefficient $C_D$) was increased by a factor of 220 percent at a towing speed of 4.25 knots. At this and nearby towing speeds, the cross flow displacement amplitude of the cylinder was $\pm 1.5$ to 2 diameters (25). When the cylinder was towed at speeds above and below the resonance, the usual

$$\text{Drag} \propto (\text{Flow Speed})^2$$

dependence was obtained. Methods for calculating the steady drag-induced deflections that accompany vortex shedding are discussed in the next section of the paper. Details of the method and extensive comparisons with the experimental results plotted in Figure 7 are given by Griffin (6) and by Every, King and Griffin (26).

The measured drag coefficients ($C_D$) for several strumming cables are plotted against the Reynolds number ($Re$) in Figure 9. As a basis for comparison the typical drag coefficients for a stationary circular cylinder and several nominally stationary braided and plaited marine cables also are plotted in the figure. The relatively large scatter in the stationary cable data is due to variations in the low cable tension values at the lowest flow speeds (Reynolds numbers). All of the cable strumming experiments were conducted in one of the towing channels at the DTNSRDC. The strumming test rig is described

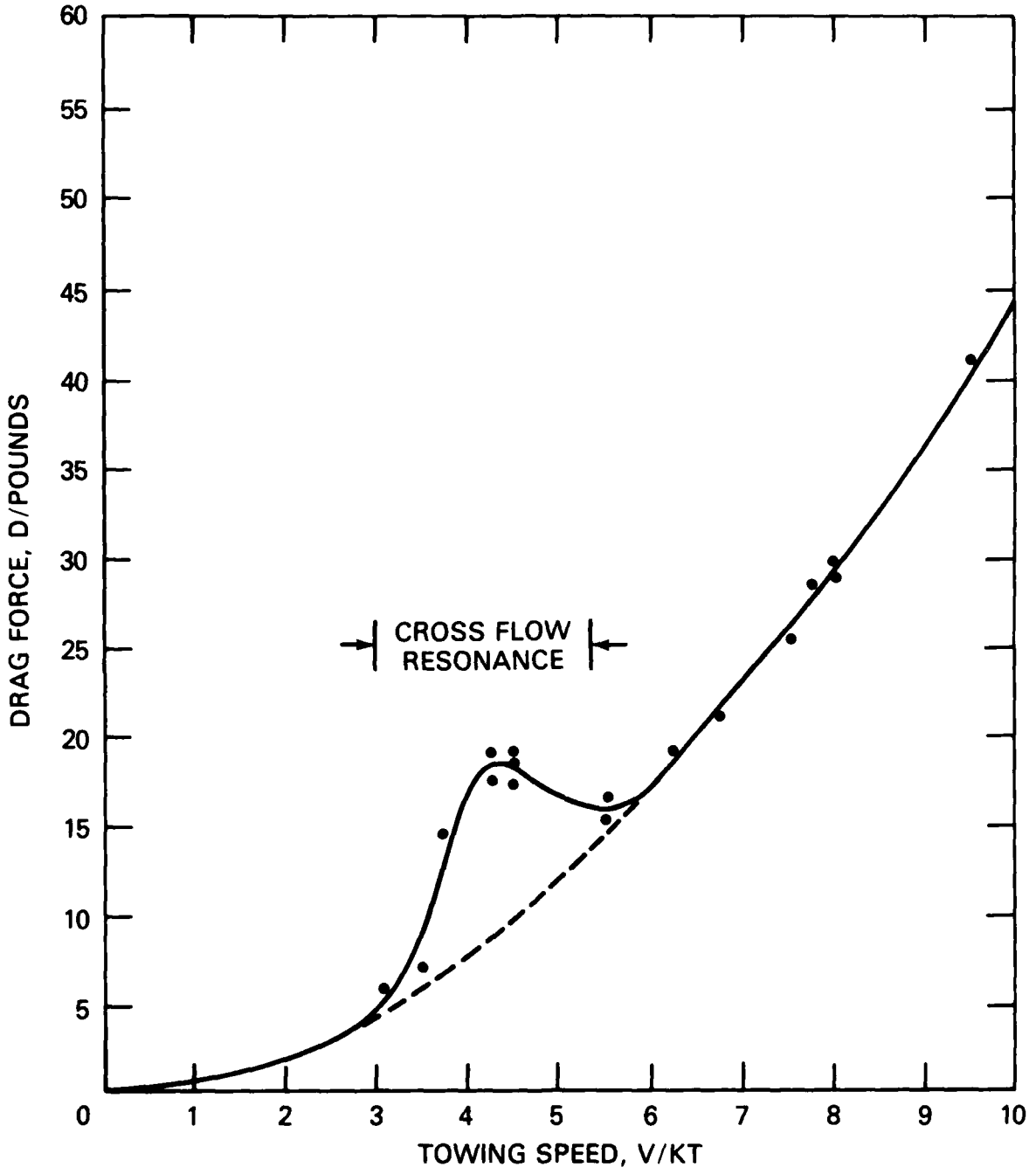


Fig. 8 – Steady drag force measured on a free-ended circular cylinder towed through still water. A clear resonance in the drag due to vortex-excited oscillations perpendicular to the incident flow is shown between relative flow speeds of $V = 3$ and 6 knots; from Grimminger (25).

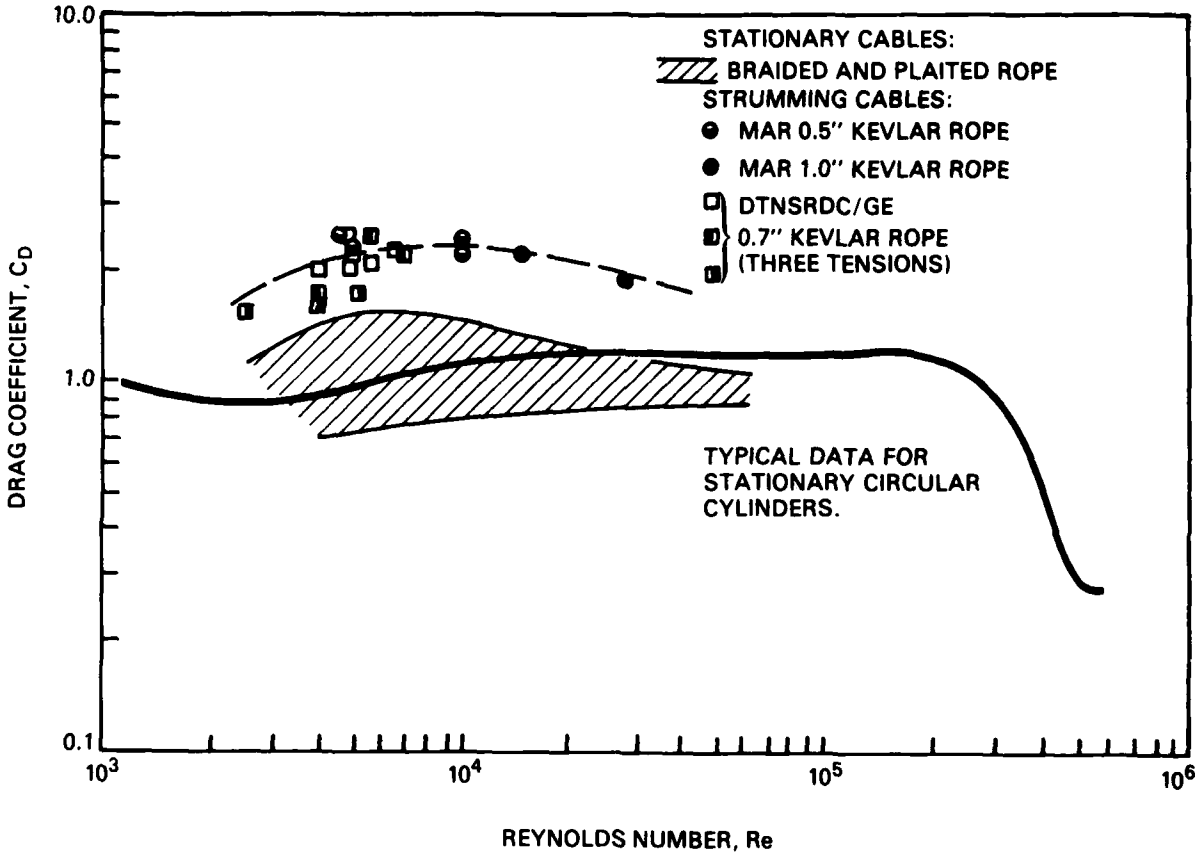


Fig. 9 — The drag coefficient $C_D$ plotted against the Reynolds number $Re$ for several synthetic fiber marine cables. A curve of $C_D$ versus $Re$ for typical stationary cylinders is plotted as a reference. All of the cable strumming experiments were conducted at the David Taylor Naval Ship R&D Center. The original figure was provided by D.J. Meggitt of the Naval Civil Engineering Laboratory.

in several papers and reports (2,27,31) and is shown in Figure 14. It is clear that the drag coefficients $C_D$ for the strumming cables are increased substantially (by as much as a factor of two) for a variety of Kevlar cables over a wide range of towing speeds or Reynolds numbers between $Re = 3(10^3)$ and $3(10^4)$. This steady drag increase is typical of structures and cables that resonantly vibrate due to vortex shedding.

*3.1.4 Other factors.* A number of factors influence the process of vortex shedding and vortex-excited oscillations from bluff cylinders. These factors include the surface roughness, Reynolds number effects, shear and turbulence in the incident flow, and coherence of the vortex shedding along the span of the structure. Also of importance is the influence of yaw or inclination of the cable or cylinder away from normal incidence to the flow. These factors are discussed in detail by Griffin and others (2,5,27).

### 3.2 Laboratory-Scale Cable Strumming Experiments

*3.2.1 Cable response in a flowing fluid.* The measured frequency and displacement amplitude responses for small-diameter taut cables undergoing cross flow strumming vibrations in water are plotted in Figures 10 and 11. These results are taken from laboratory-scale experiments reported by Dale, Menzel and McCandless (28). In the first set of experiments (see Figure 10) a 2.5 mm diameter cable, 0.9 m in length, was excited in three resonant strumming modes over the frequency range 14-28 Hz, and in the second set of experiments (see Figure 11) a cable of the same diameter, but 1.8 m in length, was excited in six modes over the same frequency range. Predictions have been made for the response frequency and the strumming displacement for the case shown in Figure 10 and they are shown there as a function of the flow speed $V$ together with the experimental results obtained by Dale and his colleagues. The calculations of the cable response were made with the "wake-oscillator" model of Skop and Griffin (16). The agreement between the prediction and the experiments is generally satisfactory for the strumming displacement and frequency, the flow speed at the maximum amplitude and the flow

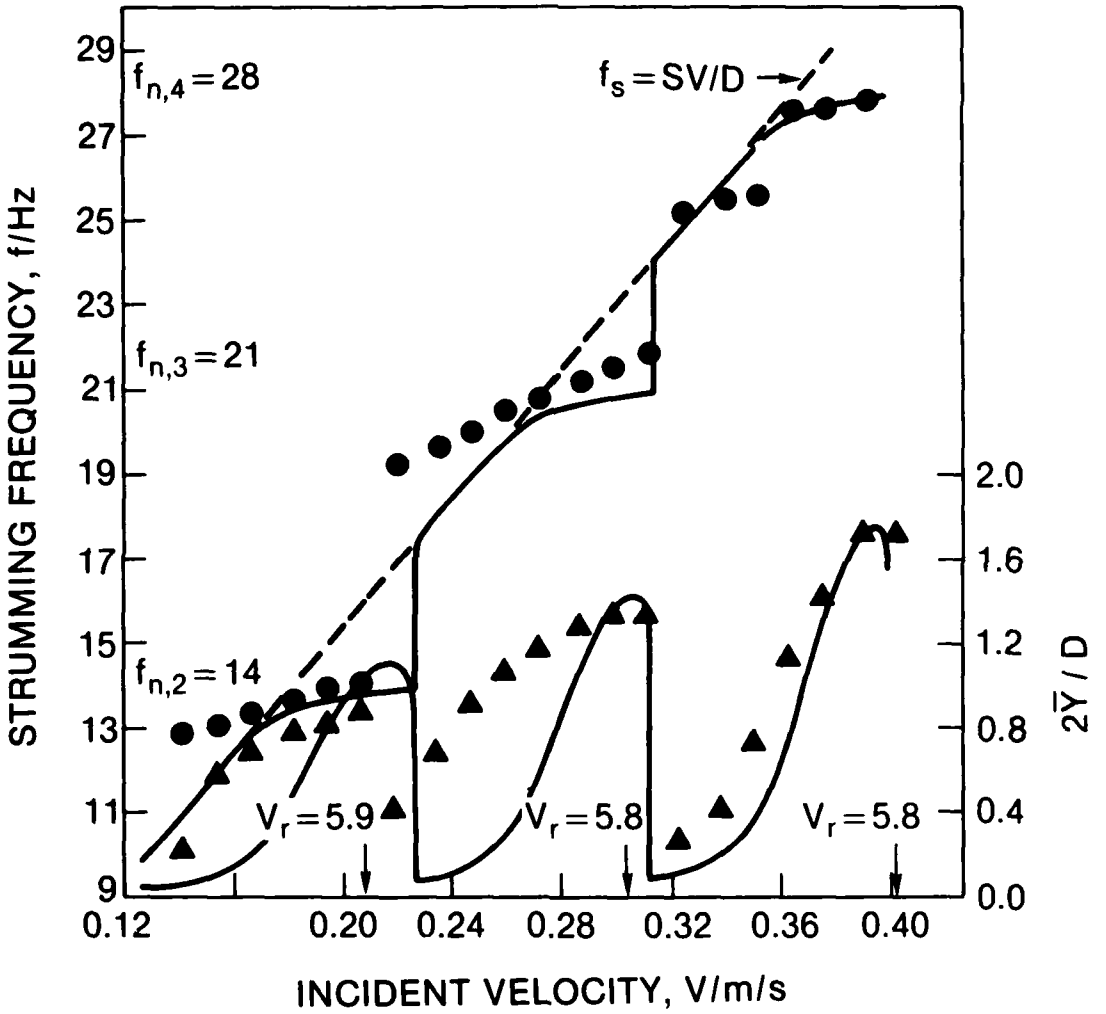


Fig. 10 – Vortex-excited strumming vibrations of a taut marine cable; from Dale, Menzel and McCandless (28)

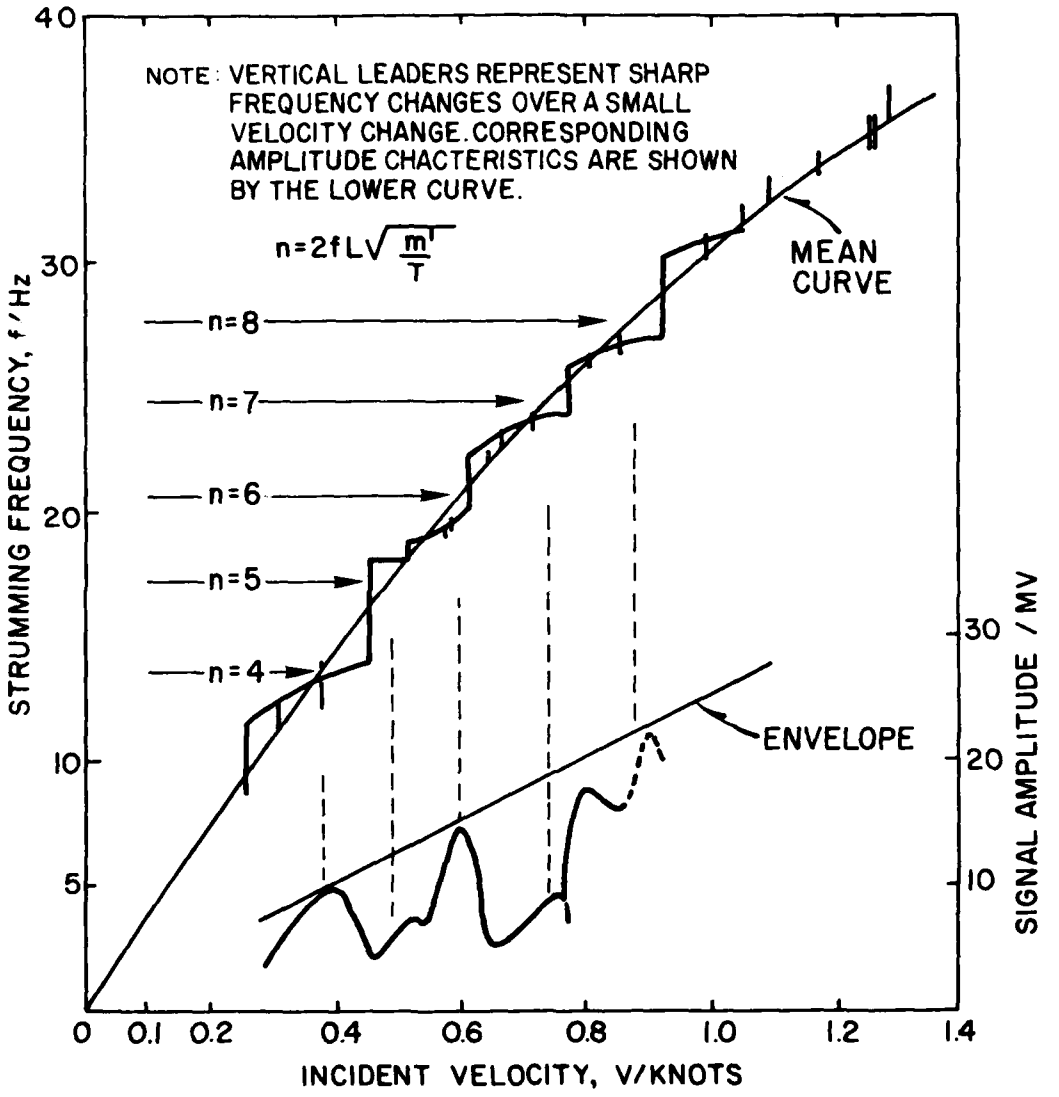


Fig. 11 — Vortex-excited strumming vibrations of a taut marine cable; from Dale Menzel and McCandless (28)

speeds at which the cable passes from one natural mode to the next. The reduced velocities which correspond to the peak strumming displacements are noted on the figure. The higher modes and frequencies of the cable result in larger strumming displacements. This follows from the dependence of the cable's damping ratio $\zeta_s$ on 1/f, which results in smaller values of the reduced damping at the higher frequencies and, consequently, larger strumming amplitudes.

The steady drag and the tension fluctuations on a strumming small-diameter cable were measured by Dale and McCandless (29). The cables employed in the experiments were between 1.45 mm (0.057 in) and 3.6 mm (0.140 in) in diameter and approximately 0.9 m (3 ft) long. A spherical mass of 0.23 kg (0.5 lb) was attached to the free end of the cables as they were towed through still water. The details of the experimental set-up are discussed by Dale and McCandless. The drag and strumming force (fluctuating tension at the attachment) are plotted in Figures 12 and 13. The tests were conducted with a smooth cable 2.72 mm (0.107 in) in diameter. The third ($n = 3$) and fourth ($n = 4$) mode resonances of the cable are clearly shown as the relative flow velocity (Reynolds number) is increased. A portion of the second mode ($n = 2$) is visible at the left-hand side of both figures. The drag coefficient $C_D$ is amplified for all of the modes from the stationary cable reference value plotted in the figure. The peak value of the tension fluctuation for each cable mode corresponds to the peak strumming displacement amplitude and to the peak drag coefficient for that particular cable mode. In other experiments conducted as part of the same program, Dale and McCandless measured strumming drag coefficients as large as $C_D = 2$. This corresponds to an amplification of the steady drag by a factor of about two, a finding which is in good agreement with the results discussed elsewhere in this report.

*3.2.2 Towing and flow channel experiments.* A program of cable strumming experiments was carried out in the towing channel at the David W. Taylor Naval Ship R&D Center (DTNSRDC) (2,27,30,31). These experiments added more details concerning the behavior of flexible cables to the fundamental results that are described earlier in this report.

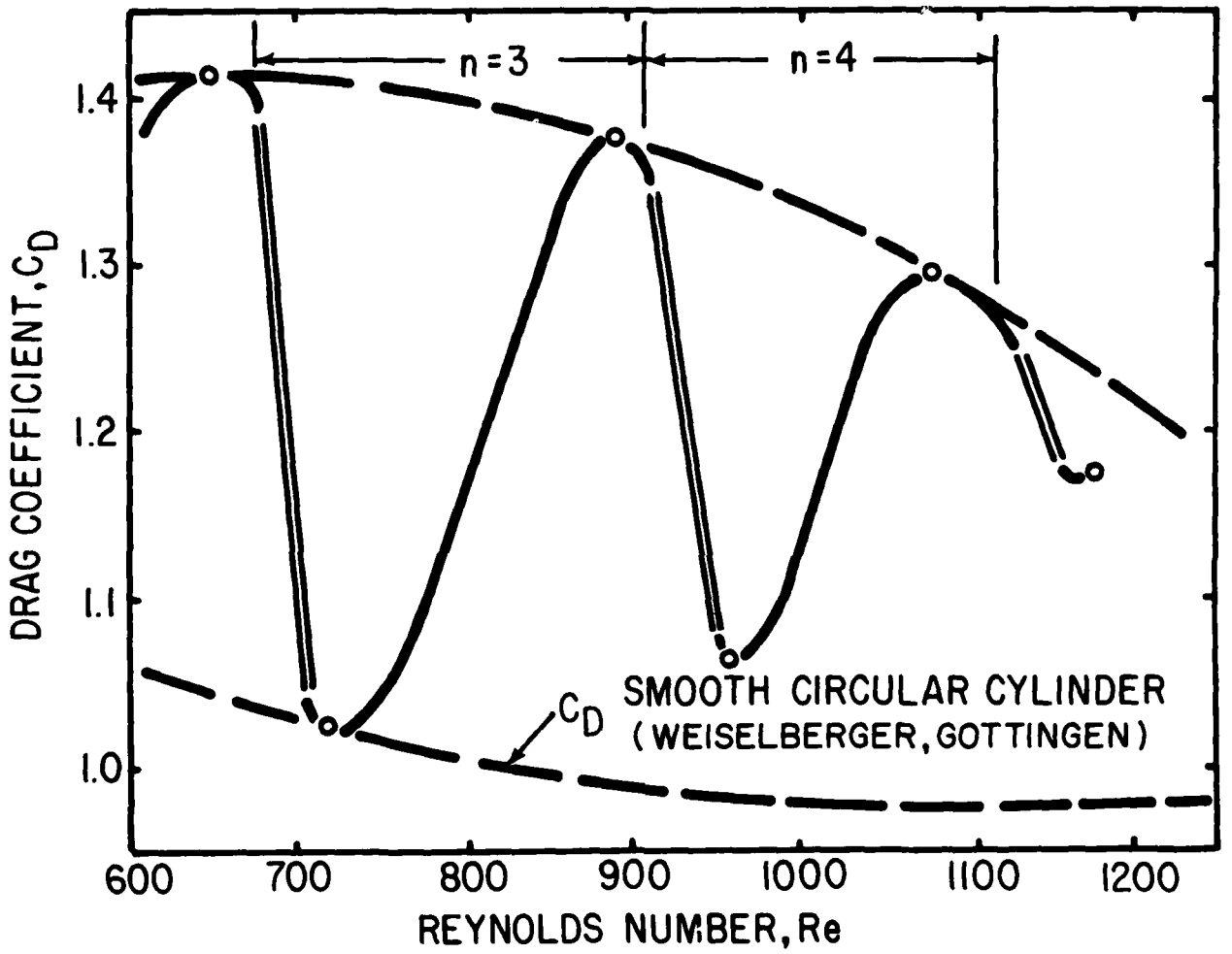


Fig. 12 — Strumming drag coefficient $C_D$ for a smooth cable plotted against the Reynolds number Re; from Dale and McCandless (29)

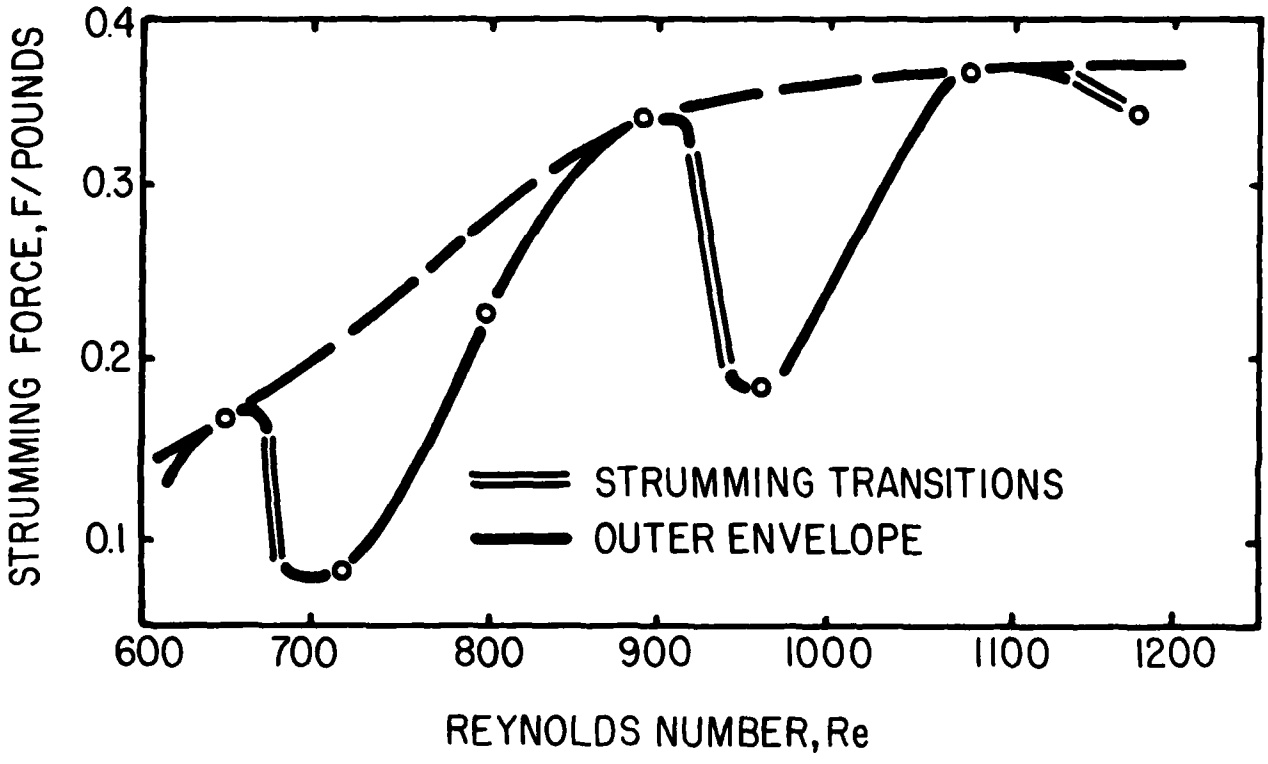


Fig. 13 — Strumming force (tension fluctuation)$^2$ for a smooth cable plotted against the Reynolds number; from Dale and McCandless (29)

Three models (Double Armor Steel, Uniline, and Small Diameter Cables) were fabricated to vary the cable density and length-to-diameter ratio; the physical characteristics of the models are listed in Table 3. A rotatable twin strut assembly was used in which cables up to 4.4 m (14.5 ft) in length could be held at static tensions up to 2225N (500 lb) and towed at speeds up to 2.5 m/s (5 kt) at various angles to the tow direction between $\theta = 0$ and 90°. A line drawing of the test platform is shown in Figure 14. Two sensors were used to measure displacements at selected points along the cable. Each sensor consisted of two sets of electric dipoles, which were set 89 mm (3.5 in) apart; these were used to sense the position of the cable in terms of two vector signals. In later analysis of the data, the horizontal and vertical displacements were derived from the dipole signals. The accuracies obtained in the measurement and analysis processes were calculated and are discussed in detail together with equipment and data analysis techniques by Pattison (30).

The data from the DTNSRDC towing experiments are discussed in detail by Griffin et al (2,27). These experiments reveal a number of interesting phenomena relating to the dynamics of both taut and slack marine cables. Several test runs were conducted with the Double Armor Steel Cable at a relatively low tension, $T = 289$N (65 lb); this condition corresponds to a slack cable (see reference 2). The critical tension $H$ below which slack cable effects become important is given by the equation

$$H_{crit} = 0.93\ (W^2EA)^{1/3},$$

where $W$ is the *total* weight of the cable in water, $E$ is Young's modulus of the cable material and $A$ is the cable's cross-sectional area. These parameters are all known for the case of the Double-Armored Steel (DAS) cable.

Table 3
Cable Model Physical Characteristics;
DTNSRDC Experiments

| Model | Diameter mm | Length m | Weight, N/m | |
|---|---|---|---|---|
| | | | In Air | In Water |
| Double Armored Steel (DAS) | 15.5 | 4.38 | 7.59 | 5.71 |
| Uniline | 15.2 | 4.35 | 2.77 | 1.01 |
| Small Diameter | 1.77 | 4.34 | 0.095 | 0.070 |

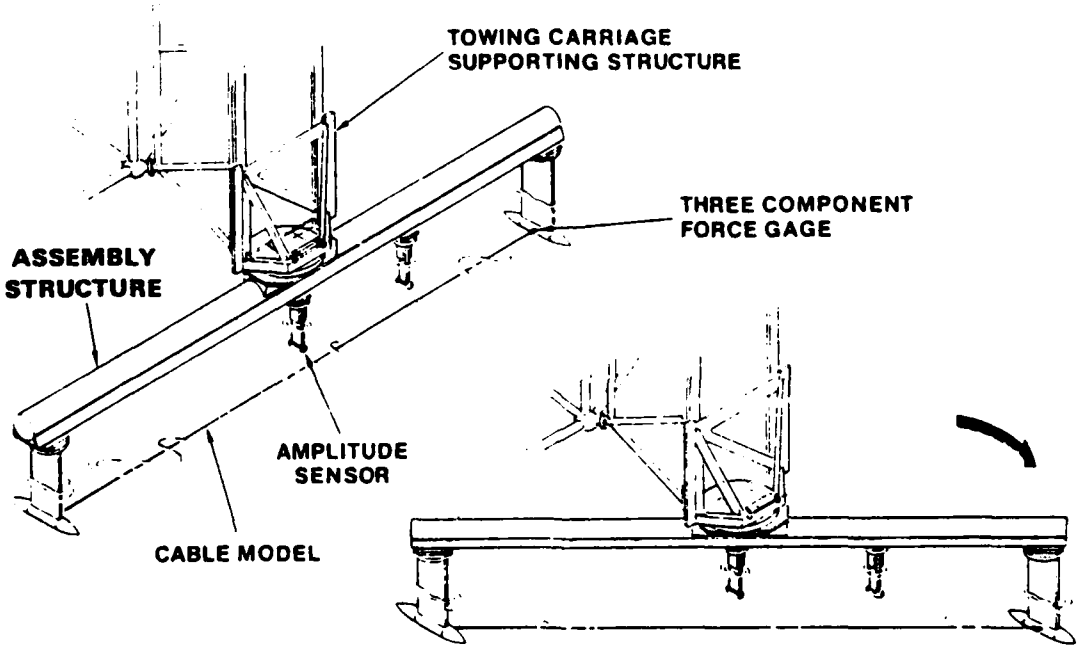


Fig. 14 — A line drawing of the DTNSRDC experimental strumming test rig; from Griffin et al (27)

The computed and measured natural frequency-tension behavior is shown in Figure 15. The critical tension $H_{crit}$ is in the range 756 to 1112N (170 to 250 lb) based on the $EA$ values given in the figure, so that the conditions for several test runs fell within the slack cable regime. The natural frequency of the DAS cable in water is $f_n$ = 4.2 Hz, which falls within the frequency "crossover" range enclosed by the dashed lines in the figure. This modal crossover is a complex phenomenon associated with the dynamics of slack cables with small sag-to-span ratios. At the crossover *three* modes of the cable have the same natural frequency and include a symmetric in-plane mode, an anti-symmetric in-plane mode and an out-of-plane or sway mode. The symmetric modes contain an even number of nodal points along the cable while the anti-symmetric modes contain an odd number of nodes.

It is sufficient to note here that although these results fall within this complex regime, *the transverse vibration amplitudes for these runs are comparable to those measured under taut conditions.* The strumming waveform contains an appreciable in-line component at the *transverse vibration* frequency and there are large phase differences between the in-line and transverse components. Small or non-existent phase differences were exhibited during the taut cable strumming experiments.

The displacements amplitudes for several runs are plotted in Figure 16 as a function of the reduced velocity $V_r = V \sin \theta / f_n D$, where the normal velocity component incident to the cable is given by $V \sin \theta$. (The legend on the figure lists the tension, inclination angle, structural log decrement, and the reduced damping $k_s$ for the three cables.) Each run corresponds to a resonant, vortex-excited response over the lock-on regime between the vortex shedding and cable vibration frequencies. In the first mode ($n$ = 1) results shown in Figure 16, all three cables exhibit nearly the same maximum strumming displacement at $V_r \approx 6$, which is typical of vortex-excited oscillations of cables and bluff structures as shown by the results in Figure 1. The peak displacements are slightly lower than one might expect from the limiting values at low damping in Figure 3, but the measured strumming frequencies in Figure 16 clearly show the constant frequency vs. flow velocity resonance (lock-on) that characterizes vortex-excited oscillations.

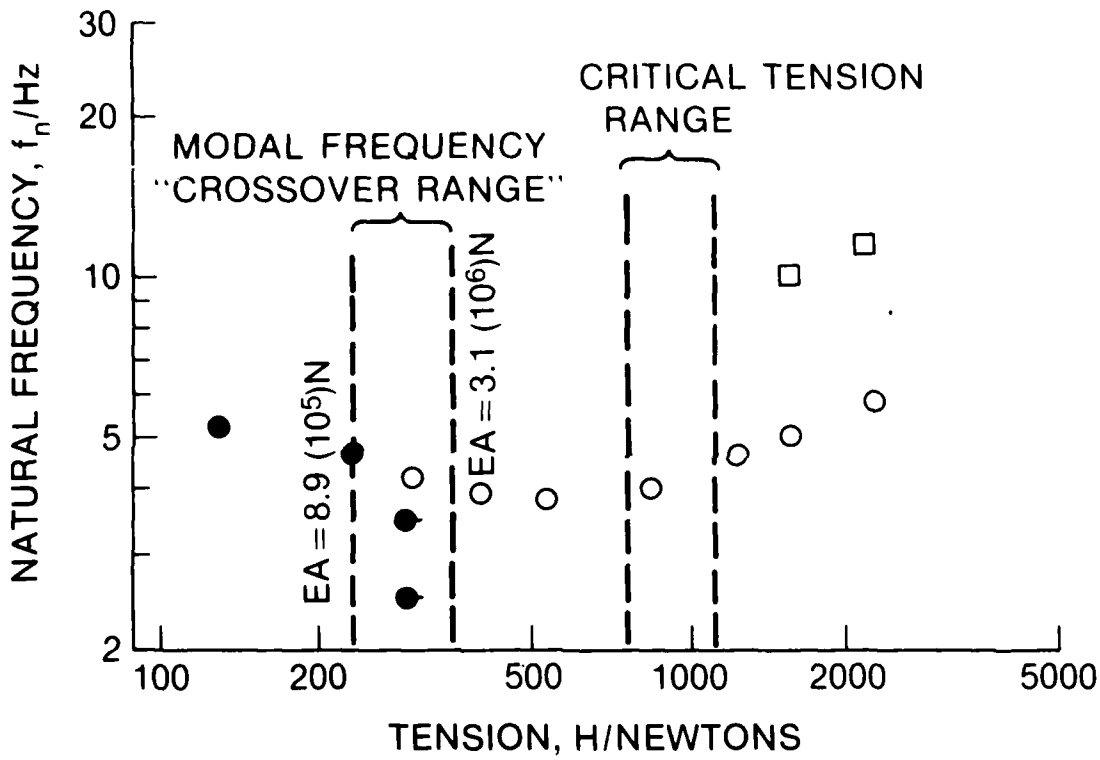


Fig. 15 — The measured vibration frequencies of a Double-Armored Steel cable in water as a function of the tension; from Griffin et al (27)

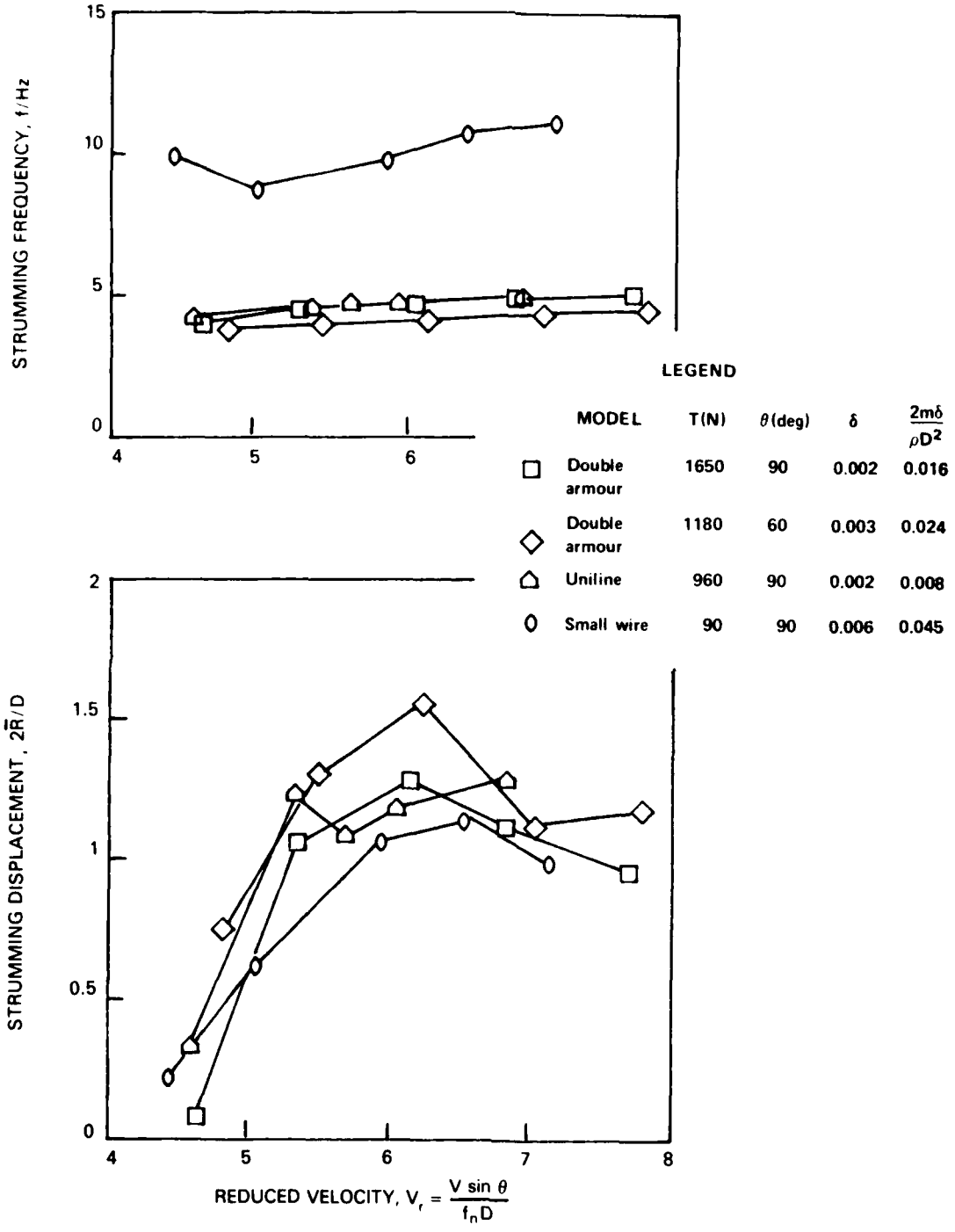


Fig. 16 — Strumming displacements and frequencies of marine cables in the fundamental mode; from Griffin et al (27)

A program of experiments was conducted to investigate the effects of sensor housings (attached discrete masses) on the overall cable response. A report on the results obtained has been given recently by Kline, Fitzgerald, Tyler and Brzoska (32). Some of these results are summarized briefly here and compared with the results shown in Figure 16. The tests were conducted on the same "strumming rig" at the DTNSRDC that was employed in the strumming experiments discussed above.

Some of the results obtained during these experiments are plotted in Figure 17. The attached masses in all cases were one or two aluminum sensor housings attached at various locations along the 4.57 mm (0.18 in.) diameter steel cable span of 4.42 m (14.5 ft). It can be seen from the results in the figure that the cable was tested at various conditions in the resonant, cross flow strumming regime during the experiments. *The attached masses did not deter or diminish the strumming,* but instead the system consisting of a bare cable plus attached masses reached higher cross flow displacement amplitudes than the bare cable alone. The conditions of MAR's bare cable reference experiment were at the onset of the resonant strumming regime while the attached mass experiments reached well into the resonant region as shown in Figure 17. All of the tests were conducted in the range of cable and attached mass properties where hydrodynamic effects dominate (the left-hand portion of Figure 3), and even the addition of concentrated masses does little to deter large-displacement cross flow strumming effects. All of the frequency spectra plotted by Kline et al (32) give clear evidence of cross flow strumming at a single resonant frequency.

### 3.3 Field Measurements of Cable Strumming

*3.3.1 Small scale field experiments.* Field studies of the strumming behavior of marine cables were conducted over several summers through 1981 at Castine Bay, Maine by staff members of the Ocean Engineering Department at MIT. The field test layout is shown in Figure 18. Sections of faired and unfaired cables, nominally 23 m (76 ft) in length, were positioned normal to a spatially uniform tidal current which ranged in magnitude from 0 to 0.7 m/sec (0 to 1.36 kt). The earlier experiments were reported in detail (33). Some more recent experiments, performed during 1976, were concerned with

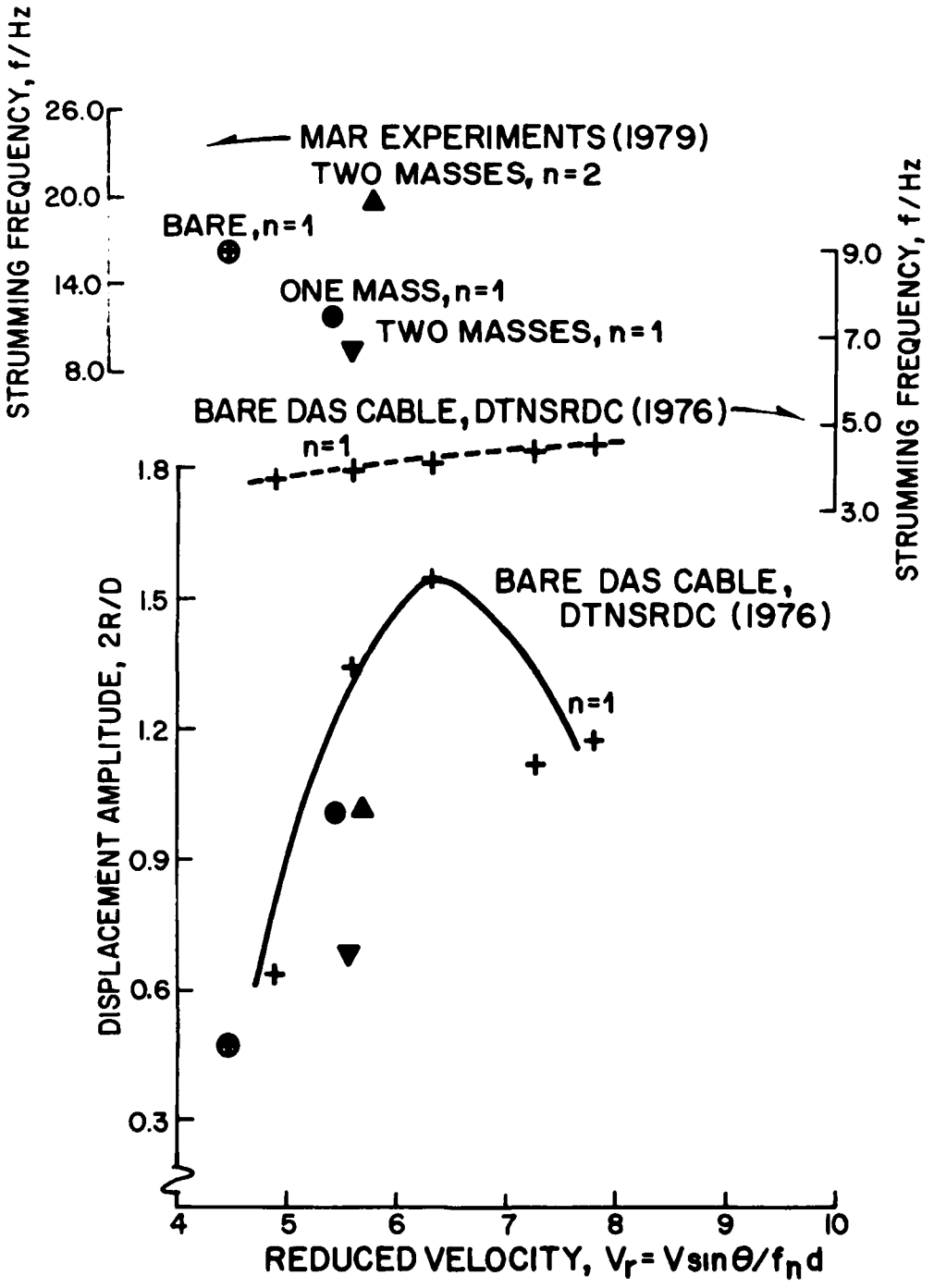


Fig. 17 — Strumming displacement amplitudes for cables with attached sensor housings; experimental data from Kline et al (32), figure from Griffin et al (2)

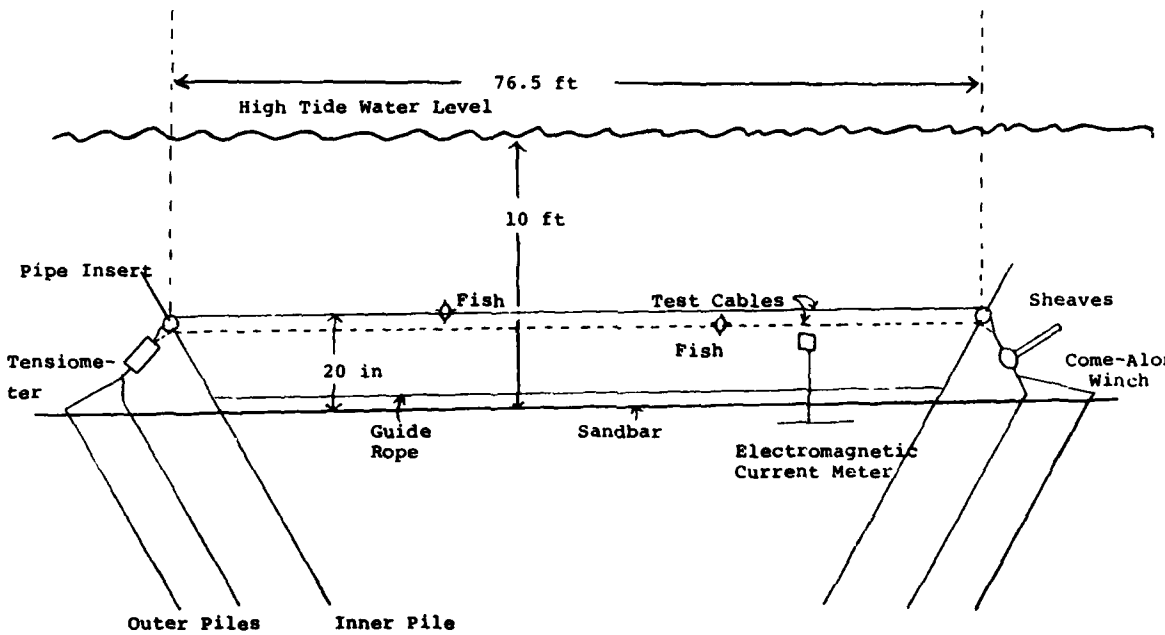


Fig. 18 — Layout of the Castine Bay cable strumming test set-up; from Griffin et al (2)

detailed measurements of the strumming response of both unfaired and faired marine cables in an ocean environment (34). As with the DTNSRDC cables, measurements of the natural frequencies (in-air and in-water), the added mass, and the fluid dynamic damping of the cables were made at NRL and are discussed in reference 2. The most recent experiments were conducted at Castine during the summer of 1981, and a discussion of some preliminary data reduction for these experiments is given at the end of this section.

The strumming behavior of the cables tested during these experiments has been classified into three general categories: resonant lock-on, non-resonant lock-on and non-lock-on. The first of these categories, resonant lock-on, is characterized by very stable motion of the cable in one of its natural modes where the displacement is sinusoidal and the displacement amplitude is essentially constant. Non-resonant lock-on is characterized by small modulations in the cable vibration displacement and frequency. These two lock-on regimes are shown in Figure 19 where two data records from the Castine Bay experiments are plotted. Non-lock-on occurs when the natural vortex shedding frequency is just outside of the synchronization range. The results obtained in this latter regime are discussed in a recent paper by Kennedy and Vandiver (35).

The results from the Castine Bay experiments that pertain to the case of resonant lock-on now are discussed. The actual vibration frequencies measured at currents between 0.2 and 0.6 m/sec (0.4 and 1.2 kt) with an unfaired Kevlar cable positioned in the tidal flow are plotted in Figure 20. The tension changed slightly (less than 5 percent) during the run time, so that the measured frequencies are scaled here by [Tension]$^{1/2}$ in order to account for the slight variations in the natural frequencies of the cable. When this adjustment is made, the natural modes of the Kevlar cable are clearly highlighted as shown in Figure 20. Five natural modes ($n$ = 3 to 7) also are shown in the figure. The mode numbers were estimated from the taut cable equation

$$n \approx 2Lf_n\sqrt{\frac{m'}{T}} \tag{8}$$

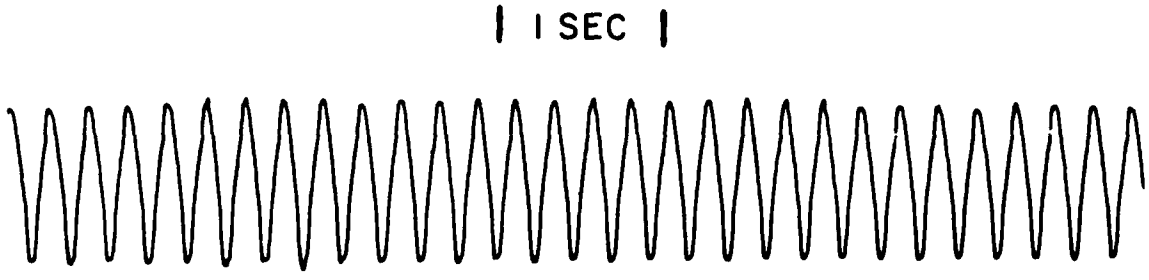


(a) RESONANT LOCK-IN.

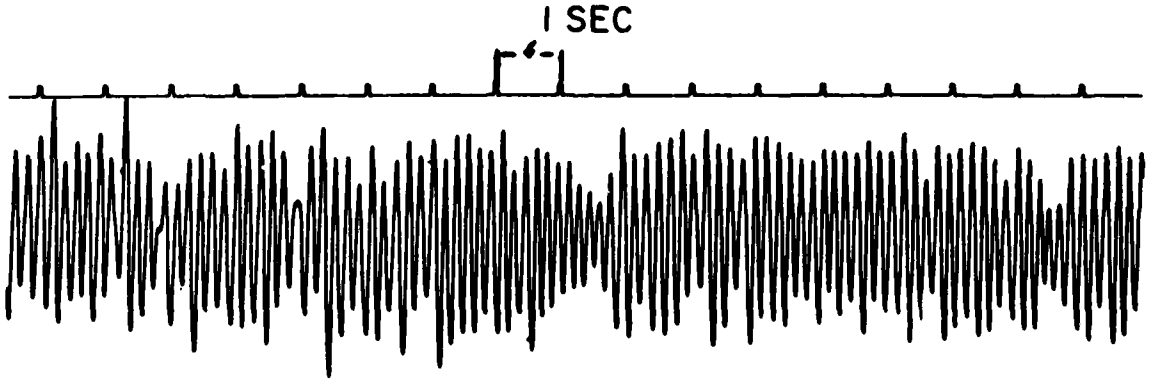


(b) NON-RESONANT LOCK-IN.

Fig. 19 – Sample displacement amplitude signal traces in the resonant and non-resonant lock-on regimes; from Griffin et al (2)

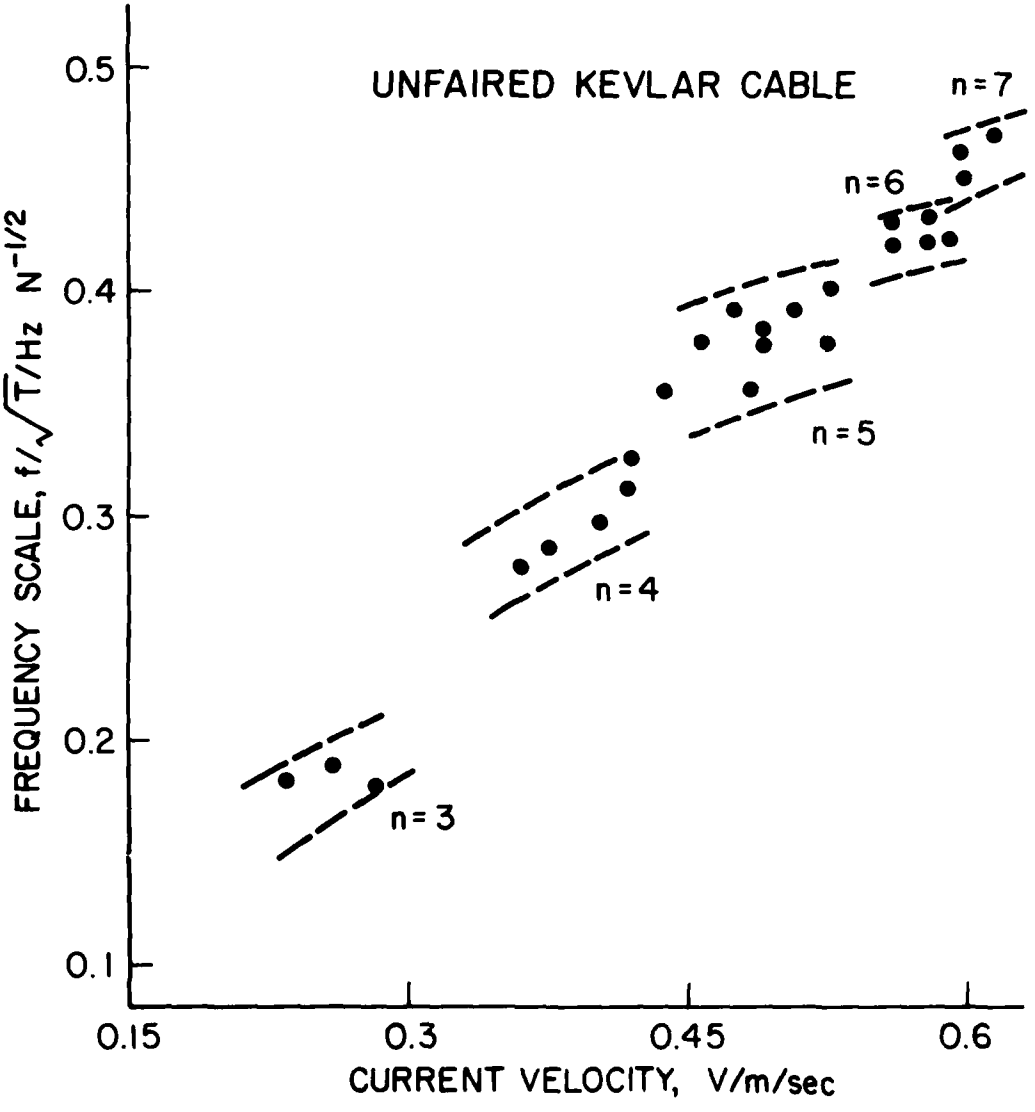


Fig. 20 — Measured resonant frequencies of cable strumming in the ocean plotted against the tidal current speed; from Griffin et al (2)

after taking into account the added mass of the cable. The frequency response of these relatively long cables (23 m or 76 ft) is similar to the strumming response of a meter-long cable employed by Dale, Menzel and McCandless (28) in their small scale experiments discussed in Section 3.2.1. The strumming response of the short sample of cable is shown in Figure 10; the similarities between the field and the laboratory are evident.

An experimental test program was conducted at the Castine field site during the summer of 1981 to provide a more extensive data base for the strumming response of marine cables and flexible cylinders under controlled conditions. A study was made of the hydroelastic response of a long cable (22.9 m or 75 ft) with and without attached sensor housings and of a flexible cylinder of the same length. The cable with a 32 mm (1.25 in.) diameter contained seven pairs of biaxial accelerometers that were placed at various spanwise locations to provide a detailed history of the overall strumming response. The cable consisted of an outer jacket and three 3.2 mm (0.125 in.) steel cables that provided strength in tension. The volume not taken up by the small cables and the accelerometers and their connecting leads was filled with an epoxy potting compound to insure that the cross-section of the overall cable assembly remained circular. The cylinder was assembled by fitting a thin-walled shell 41 mm (1.6 in.) in diameter over the cable and so the array of accelerometer pairs also was used to record the cylinder response. Additional data acquired at the test site included current velocity (two locations), cable tension and the hydrodynamic drag force.

A time history of the cable drag coefficient $C_D$ and the current velocity $V$ are plotted in Figure 21. The data are taken from a typical test run with the cable only and no attached sensor housings. From the approximately 35 minutes of data recorded with the cable strumming it is clear that the hydrodynamic drag is increased consistently from the level that is typical of a stationary cylinder or cable ($C_D$ = 1 to 1.5). The measurements of $C_D$ are consistently between 2 and 3 for the time interval shown the current velocity is near 0.6 m/s (1.2 kt). It was observed at the test site that the strumming response of the cable was in the first six (n = 1 to 6) natural modes (36).

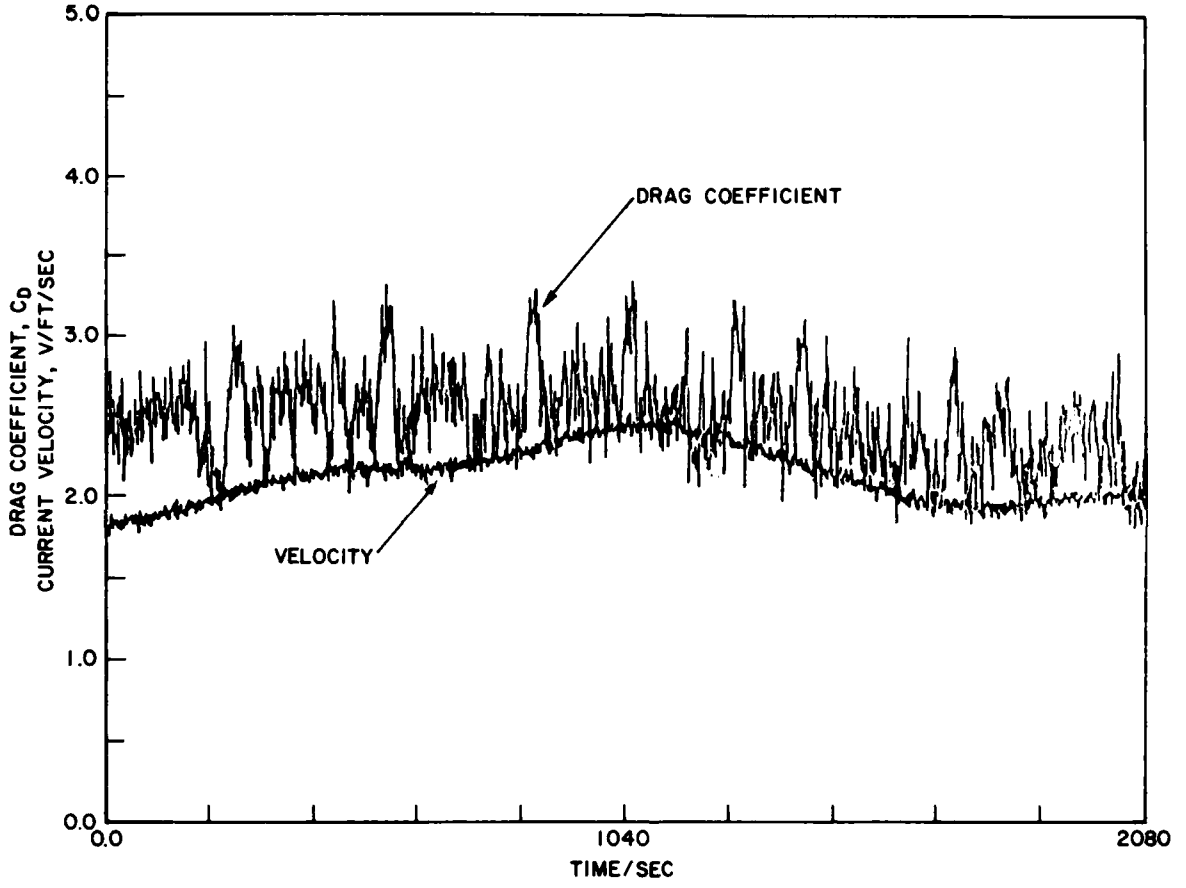


Fig. 21 — A time history of the drag coefficient $C_D$ and the current velocity $V$ recorded during a cable strumming field test program conducted during 1981. Cable length $L$ = 22.9 m (75 ft), cable diameter $D$ = 32 mm (1.25 in.), specific gravity $SG$ = 1.3. The original figure was provided by Dr. J.K. Vandiver of MIT.

Similar measurements were made using the cylinder and very similar levels of $C_D$ were obtained. Time histories of the cylinder response showed that displacement amplitudes of up to $\overline{Y}/D = \pm 1$ were obtained under conditions of resonant lock-on when the cylinder vibrations were excited in the third (n = 3) mode by the vortex shedding (36).

*3.3.2 Large scale field experiments.* FISHBITE is the name of a marine cable experiment conducted by Softley, Dilley and Rogers in 1976 (37). A wire rope 12 mm (0.47 in.) in diameter and 500 m (1640 ft) long was hung from a ship anchored in 1960 m (6430 ft) of water at the Tongue of the Ocean, located at 77° 52′ W and 25° 10′ N. The tidal flow varied both temporally and spatially from 0.1 to 0.4 m/s (0.2 to 0.8 knots). A current meter was attached at the halfway point, but no other lumped masses were attached to the cable. The cable response was measured at the top end only and the cable parameters resulted in a modal spacing of 0.025 Hz.

The response typically included more than one hundred modes between 8 and 12 Hz, with a center frequency of 10 Hz. From a study of the data from this experiment Kennedy and Vandiver (35) have noted that the rms response at the measurement point on the upper end of the cable was limited to less than one cable diameter. They attribute the bandwidth of the cable response to spatial and temporal variations of the current at the test site. No lock-on was observed during any of the FISHBITE experiments.

SEACON II was a major undersea construction experiment which had as its goal the measurement of the steady-state response of a complex three-dimensional cable structure to ocean currents. The measured array responses were to be employed in a validation of analytical cable design models and computer codes (38). A second goal of the SEACON II experiment was to demonstrate and evaluate new developments in ocean engineering which were required to design, implant, operate, and recover fixed undersea cable structures.

The SEACON II structure consisted of a delta-shaped module with three mooring legs. It was implanted in 885 m (2900 ft) of water in the Santa Monica Basin by the Civil Engineering Laboratory

during 1974 and was retrieved during 1976. The top of the cable structure was positioned 137 m (450 ft) below the water surface. The mooring legs were 1244 m (4080 ft) long and each arm of the delta was 305 m (1000 ft) long. An artist's view of the completed structure is shown in Figure 22. Two mooring legs were attached to explosive anchors embedded in the sea floor and the third leg was attached to a 5680 kg (12500 lb) clump anchor. The entire cable structure was instrumented in order to collect water current and array position data.

The data were used to validate the computer code DECEL1 (the NRL version is called DESADE). This code was developed at NRL (39) and is discussed in Section 5 of this report. The delta cables experienced uniform currents over their respective lengths and often were subject to cable strumming. These strumming oscillations led to increased steady drag coefficients and static deflections as discussed further in Sections 2 and 3 of this report and by Skop, Griffin and Ramberg (23). Details of the SEACON II implantation, design and recovery are given by Kretschmer, Edgerton and Albertsen (38).

The drag coefficient $C_D$ of the SEACON II cable was measured in two series of tests conducted for CEL. These measurements are plotted in Figure 23. The tests conducted at the Naval Postgraduate School utilized a short segment of the cable that was restrained from oscillating. An average value of $C_D = 1.55$ was obtained. The DTNSRDC tests were conducted with a 4.6 m (15 ft) long cable segment. The resonance in the drag versus Reynolds number data in Figure 23 was caused by cable strumming. The drag resonance is similar to that measured by Grimminger (25), Dale and McCandless (29) and others and plotted in Figures 8, 9 and 12.

A cable strumming experiment (the Bermuda Testspan) was conducted by the U.S. Navy from December 1973 to February 1974. The site of the experiment was near Argus Island, Bermuda. A 256 m (840 ft) long, 16 mm (0.63 in.) diameter electromechanical cable was suspended horizontally in the water at a depth of 28 m (92 ft). The cable had no strumming suppression devices attached, but it had numerous weights, instrumentation devices, and floats distributed over its length. The unfaired cable

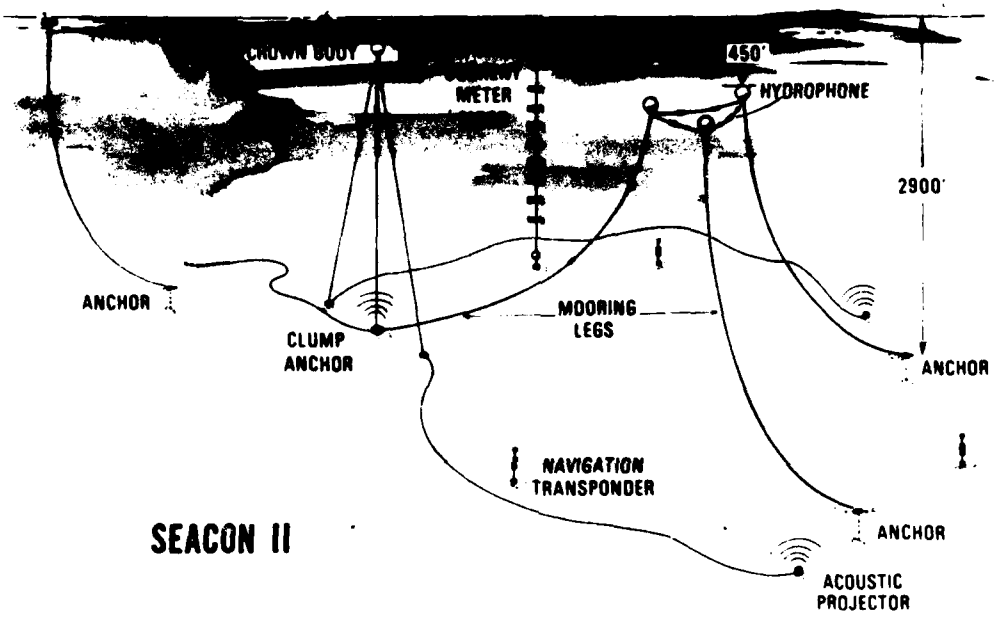


Fig. 22 — A schematic drawing of the SEACON II experimental cable mooring

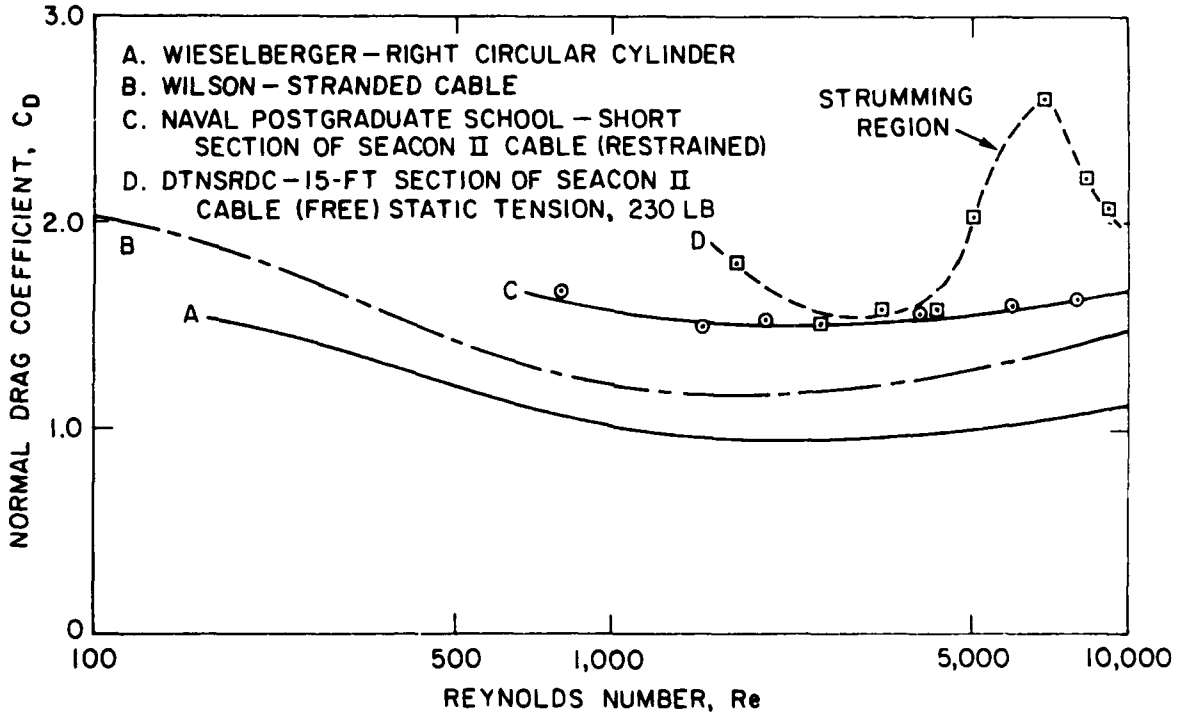


Fig. 23 — Measured drag coefficients for the SEACON II cable; from Kretschmer et al (38)

and instrumentation were similar to the cables which made up the horizontal delta module of the SEA-CON II array. Two current meters were suspended near the mid-span point of the cable.

Kennedy and Vandiver (35) have analyzed the results of this experiment and have reached several conclusions. They found that the strumming response of the cable was typical of a broadband random process and that resonant and nonresonant lock-on were rare. The high modal density, which ranged from the 10th to the 150th mode, and extreme variations in current speed and direction were chiefly responsible for the broadband response of the test span. The peak rms cross flow displacement amplitude experienced by the Bermuda Testspan was estimated by Kennedy and Vandiver to be $\bar{Y} = \pm$ 0.5 D. A more thorough discussion of this large scale field experiment is given by Kennedy (40).

Alexander (41) has reported a series of experiments that were conducted with the Scripps Institution of Oceanography's Deep Tow survey system. The system, an oceanographic sensor package, was deployed from a Scripps research vessel by a towing wire 0.68 in (1.72 cm) in diameter at typical depths in excess of 6560 ft (2000 m) and at nominal towing speeds of 1.5 kt (0.75 m/s). In order to investigate suspected strumming vibrations a 2-axis accelerometer was attached to the tow wire at a depth of 98 ft (30 m) and its output was recorded in a diver-operated vehicle about 3 ft (1 m) downstream. Both in line and crossflow strumming oscillations were measured. Sharply peaked frequency spectra were obtained that contained frequencies in line at twice the crossflow strumming frequencies. An analysis of the frequency amplitude and phase data by Alexander suggests that the vortex shedding from the tow wire produces strumming oscillations in the form of travelling waves in the wire.

A towing channel fixture was built to reproduce under controlled laboratory conditions the amplitude, frequency and phase conditions of a point on the tow wire using a vibrating cylinder. A constant drag coefficient $C_D = 1.8$ was measured over a range of representative strumming conditions at Reynolds numbers in the range $Re = 7000$ at 12000. Details of the at-sea and laboratory test programs are given by Alexander (41).

# 4. STRUMMING CALCULATION METHODS

## 4.1 Analytical Models

A number of analytical models have been developed to predict the vortex-excited oscillations of general bluff cylindrical structures. Application to cable strumming problems is but one specific example of the utility of the various methods. In general the models that have been developed fall into these categories:

- Nonlinear, or wake, oscillator models;
- Empirical models, which are based upon measured fluid dynamic force coefficients;
- Random vibration models;
- Discrete vortex models, which are based upon the insertion of arrays of small vortices to represent the overall features of the vortex shedding;
- Numerical models, which are based upon numerical integration of the governing equations of fluid motion.

The wake oscillator models have been developed because many features of the resonant interaction between the vibrations and the vortex shedding exhibit the characteristics of a nonlinear oscillation. The basic idea has been developed by Skop and Griffin (16), Iwan (17), Blevins (42), and Hartlen and Currie (43), among others. The wake oscillator model most recently has been applied to marine riser vibration problems. Some limited success has been achieved as discussed by Fischer, Jones and King (24). The wake oscillator concept is discussed in detail in references 2, 16, 17 and 42.

Random vibration models to predict vortex excited oscillations in general and cable strumming in particular have been developed by Blevins and Burton (44), by Kennedy and Vandiver (35), and by Whitney, Chung and Yu (45). Some limited success has been achieved with these approaches to the

problem. A general model for employing measured force coefficients in an empirical formulation has been developed by Griffin (2,15) and Chen (21). Measured force coefficients such as those reported by Sarpkaya (14) and Griffin and Koopmann (7) are used to predict the resonant crossflow oscillations. A discrete vortex model for predicting the vortex-excited oscillations of a flexibly-mounted rigid cylinder has been developed by Sarpkaya and Shoaff (46). A numerical integration of the time-dependent Navier-Stokes equations in the presence of an oscillating cylinder has been carried out by Hurlbut, Spaulding and White (47). However this numerical scheme is limited to low Reynolds numbers, i.e. $Re < 200$, and has limited practical value. These four classes of predictive models also are discussed in detail in reference 2.

### 4.2 General Design Procedures

Design procedures and prediction methods for the vortex-excited oscillations of structures and cable systems only recently have been developed. A reliable experimental data base and accurate characterization of the phenomenon were relatively unavailable until recently, and it is only since marine construction and exploration has moved into deeper water (and more harsh operating environments) and since the requirements of oceanographers and acousticians have become more acute that the need for sophisticated design procedures has arisen. It should be emphasized, however, that reliable data are now available only at subcritical Reynolds numbers (less than $Re = 10^5$).

The design procedures that are available have been reported by Hallam, Heaf and Wootton (12), King (4), and Skop, Griffin and Ramberg (23,48). These various approaches have been unified on a common basis by Griffin (5). The methods developed by Skop, Griffin, and Ramberg have been applied primarily to the analysis of marine cable systems, though many of their basic findings have been incorporated by others in the marine industry (49). Blevins (42) discusses design problems due to flow-induced vibrations in general, including heat exchangers, overhead transmission lines, and marine structures and cables. A flowchart that describes the steps necessary to compute the amplified drag forces and steady deflections is given in Figure 24.

All of the methods developed thus far are in agreement that the following parameters determine whether large-amplitude, vortex-excited oscillations will occur (5):

- the *logarithmic decrement* of *structural* damping, $\delta$;
- the reduced velocity, $V/f_n D$;
- the mass ratio, $m_e/\rho D^2$.

Here $m_e$ is the *effective mass* of the structure which is defined as

$$m_e = \frac{\int_0^L m(x)\, y^2(x)\, dx}{\int_0^L y^2(x)\, dx} \tag{9}$$

where $m(x)$ is the mass per unit length including contributions due to internal water, fluid added mass, joints, sections of different material, etc.,

$y(x)$ is the modal shape of the structure or cable along its length,

$L$ is the overall length of the structure or cable, measured between its terminations.

The effective mass $m_e$ defines an equivalent structure whose vibrational kinetic energy is equal to that of the real structure. In the context of cable strumming, this equation is generally applicable to bare cables and to cables with distributed numbers of attached masses.

As described in the previous sections the mass parameter and the structural damping can be combined as

$$k_s = \frac{2m_e\delta}{\rho D^2} \quad \text{or} \quad \frac{\zeta_s}{\mu} = 2\pi St^2 k_s\,, \tag{3,4}$$

both of which are called the reduced damping. As noted by Hallam, et al (12), the reduced damping $k_s$ is the ratio of the actual damping *force* (per unit length) and $\rho f_n D^2$, which may be considered as an

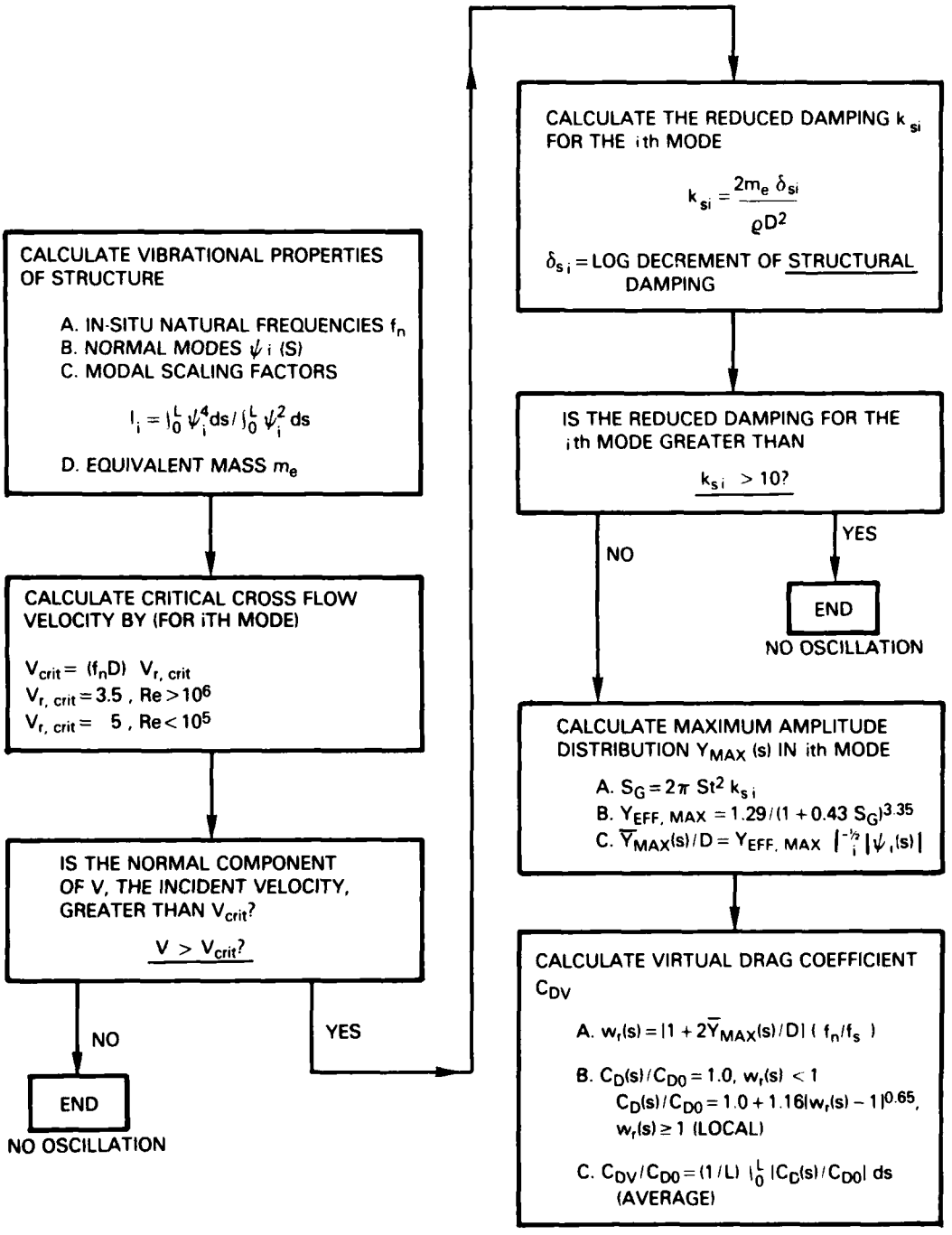


Fig. 24 — Flow diagram of the steps required for the calculation of the steady drag amplification due to vortex-excited oscillations; from Griffin (5)

inertial force (per unit length). The results in the preceding sections also suggest criteria for determining the critical incident flow velocities for the onset of vortex-excited motions. They are given by the equation

$$V_{crit} = (f_n D)\, V_{r,crit} \tag{10}$$

where $V_{r,crit} = 1.2$ for in-line oscillations and $V_{r,crit} = 3.5$ for cross flow oscillations at Reynolds numbers greater than about $5(10^5)$. For Reynolds numbers below $10^5$, $V_{r,crit} = 5$ which is a typical value for cable strumming applications.

An increase in the reduced damping results in smaller amplitudes of oscillation and at large enough values of $\zeta_s/\mu$ or $k_s$ the vibratory motion becomes negligible. Reference to Figure 3 suggests that oscillations are effectively suppressed at $\zeta_s/\mu > 4$ (or $k_s > 16$), but marine cables fall well toward the left-hand portion of the figure. The measurements of in-line oscillations by King (4) have shown that vortex-excited motions in that direction are effectively negligible for $k_s > 1.2$. The results obtained by King and by Dean, Milligan and Wootton and others shown on Figure 3 indicate that the reduced damping can increase from $\zeta_s/\mu = 0.01$ to 0.5 (a factor of *fifty*) and the peak-to-peak displacement amplitude is decreased only from 2 to 3 diameters to 1 diameter (a nominal factor of only *two or three*). At the small mass ratios and structural damping ratios that are typical of light, flexible cable arrays in water, the hydrodynamic forces predominate; it is difficult to reduce or suppress the oscillations by means of mass and damping control in that range of parameters. Typical values of $k_s$ for marine cables are given in Figure 16. Various devices and cable constructions have been developed for cable strumming suppression; these are discussed in Section 6 of this report.

Step-by-step procedures for determining the deflections that result from vortex-excited oscillations have been developed by Skop, Griffin and Ramberg (23,48), by King (4) and by Hallam, et al. (12). The steps to be taken are explained in detail in these references and generally should follow the unified sequence given most recently in references 2 and 5:

- Compute/measure vibration properties of the structure or cable system (natural frequencies or periods, normal modes, modal scaling factors, etc.).

- Compute Strouhal frequencies and test for critical velocities, $V_{crit}$ (in-line and cross flow), based upon the incident flow environment.

- Test for reduced damping, $k_s$, based upon the structural damping and mass characteristics of the structure or cable.

If the cable system or structure is vulnerable to vortex-excited oscillations, then

- Determine vortex-excited unsteady displacement amplitudes and corresponding steady-state deflections based upon steady drag augmentation according to the methods of references 5, 6, and 23, if applicable (see Figure 24).

- Determine new stress distributions based upon the new steady-state deflection and the superimposed forced mode shape caused by the unsteady forces, displacements and accelerations due to vortex shedding.

- Assess the severity of the amplified stress levels relative to fatigue life, critical stresses, etc.

### 4.3 Practical Design Data

Several dynamic models of varying levels of sophistication have been developed to predict the displacement amplitudes that are excited by vortex shedding. One class of models, the so-called nonlinear "wake-oscillator" type, have been described briefly here. More details are given in references 2, 16 and 17. None of the wake-oscillator formulations proposed thus far has been developed to the stage where it truly represents a practical procedure for detailed design of structures in both air and water, but based upon a detailed study Dean and Wootton (13) have suggested that the wake-oscillator model of Skop and Griffin (16) is perhaps the most promising for additional development. At present the wake oscillator model of has been used with considerable success in the derivation of scale factors such as those given in equations (6a) through (6c).

Several empirical predictions of the dependence between the peak cross flow displacement amplitude and the reduced damping have been developed over the past several years. The three most widely used are listed in Table 4. The prediction curve developed by Griffin, Skop and Ramberg (47) is a least-squares fit to those data points in Figure 3 that were available in 1976 (about two-thirds of the points now appearing in the figure). The Iwan and Blevins curve was developed during a study of one wake-oscillator formulation (42) and Sarpkaya's result is based upon a discrete vortex modeling study (3). The dimensionless mode shape factor $\gamma$ is given by

$$\gamma_i = |\psi_i(z)|_{MAX}/I_i^{1/2}. \tag{6}$$

Representative maximum values of $\gamma_i$ for different end conditions and mode shapes are tabulated in references 2 and 5.

All of the equations in Table 4 correctly model the self-limiting displacement amplitude that is shown at small values of reduced damping in Figure 3. It is also important to note that all of these models are based upon *the structural damping ratio*, typically *the still air value*, for whatever mode of the structure is excited. The models in Tables 4 tend to overpredict the cross flow displacement amplitude at $\bar{Y}/D < 0.05$ to 0.1 where the vortex shedding is not fully correlated over the length of the cylinder, but these small-amplitude cross flow oscillations are of more concern in gas flows rather than in water.

Table 4
*Predictions of Cross Flow Displacement*
Amplitude Due to Resonant Vortex-Excited Oscillations
as a Function of the Reduced Damping

| Investigator | Predicted Displacement Amplitude |
|---|---|
| Griffin, Skop and Ramberg (47) | $\bar{Y}/D = \dfrac{1.29\gamma}{[1 + 0.43(2\pi \mathrm{St}^2 k_s)]^{3.35}}$ |
| Blevins (42) | $\bar{Y}/D = \dfrac{0.07\gamma}{(1.9 + k_s)\mathrm{St}^2}\left[0.3 + \dfrac{0.72}{1.9 + k_s)\mathrm{St}}\right]^{1/2}$ |
| Sarpkaya (3) | $\bar{Y}/D = \dfrac{0.32\gamma}{[0.06 + (2\pi \mathrm{St}^2 k_s)^2]^{1/2}}$ |

Legend: $\bar{Y}$ = displacement amplitude; $D$ = cylinder diameter; $m$ = mass or equivalent mass per unit length; St = Strouhal number; $k_s$ = reduced damping; $\gamma$ = dimensionless mode shape factor, $\gamma = 1$ for a spring-mounted rigid cylinder, $\gamma = 1.3$ for the first mode of a cantilever, and $\gamma = 1.16$ for a sinusoidal mode shape (cable).

The drag coefficient $C_D$ for a structure vibrating due to vortex shedding is increased as shown in Figure 25. The ratio of $C_D$ and $C_{DO}$ (the latter is the drag coefficient for a cylinder, cable or other flexible bluff structure that is restrained from oscillating) is a function of the displacement amplitude and frequency as given by the response parameter (23)

$$w_r = (1 + 2\bar{Y}/D)(V_r St)^{-1}. \tag{11}$$

Here again $2\bar{Y}$ is the double amplitude of the displacement, $V_r$ is the reduced velocity and $St$ is the Strouhal number. The ratio of the drag coefficients is given by

$$C_D/C_{DO} = 1\,, \quad w_r < 1 \tag{12a}$$

$$C_D/C_{DO} = 1 + 1.16(w_r - 1)^{0.65}, \; w_r \geq 1 \tag{12b}$$

which is a least-squares fit to the data in Figure 25. The equation

$$\bar{Y}_{MAX}/D = \frac{1.29\gamma_i}{[1 + 0.43(2\pi St^2 k_s)]^{3.35}} \tag{13}$$

can be combined with equations (11) and (12) to compute the unsteady displacements, the drag amplification and the amplified static deflection that is due to the vortex excited oscillations. The local displacement amplitude along a flexible cylindrical structure (in the *ith* normal mode) is given by

$$\bar{y}(z) = \bar{Y}_i(z)\sin(2\pi ft).$$

where

$$\bar{Y}_i(z) = Y_{EFF,MAX}\, D\, \psi_i(z)/I_i^{1/2}.$$

These equations are employed as outlined in Figure 25 to iteratively compute the static deflection of a structure or cable due vortex-excited drag amplification (the drag coefficient $C_{DO}$ for the stationary cylinder or cable is assumed to be known).

Every, King and Griffin (26) recently have shown by comparison between sample calculations and the experimental data in Figure 7 that this methodology for calculating the steady drag amplification and deflections is quite accurate and can that it can be employed with some confidence to evaluate the hydrodynamic loading, deflections and material stresses on marine structures and cable systems. The *cumulative* effects of superimposed steady and unsteady loads and deflections must be considered in any

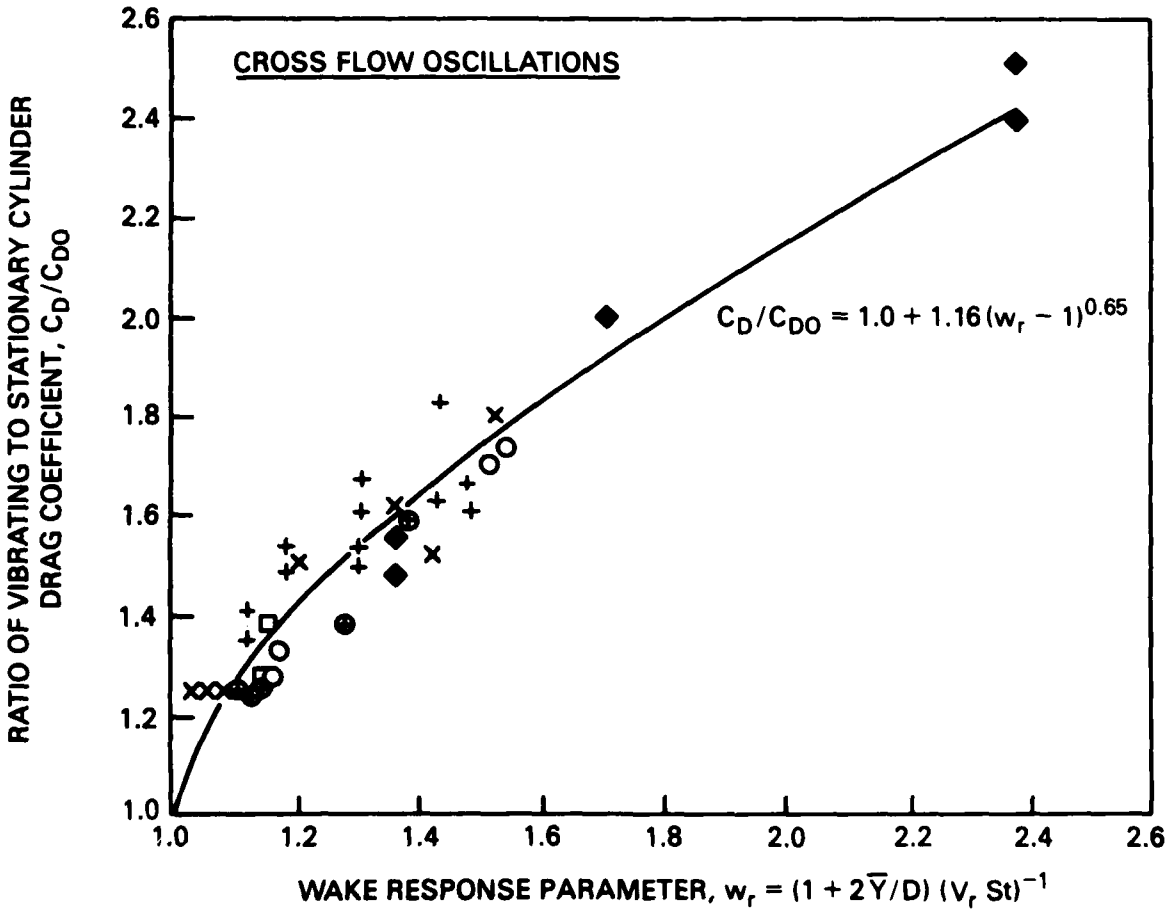


Fig. 25 — The ratio of the steady drag coefficient $C_D$ due to vortex-excited cross flow oscillations and the steady drag coefficient $C_{DO}$ on a stationary circular cylinder plotted against the wake response parameter $w_r$; from Skop, Griffin and Ramberg (23)

such evaluation. An example of the comparison reported by Every, King and Griffin (26) is given in Figure 26.

Blevins and Burton (44) have developed a random vibration model for predicting vortex-excited cross flow displacement amplitudes. The model is based upon random vibration theory in order to incorporate the effects of varying correla length on the resonant response of the structure and the flow-induced forces. The details of the model are given by Blevins and Burton (44), and will not be repeated here since the variable correlation length effects are more applicable at cross flow displacements less that $\bar{Y}/D = 0.2$ and reduced dampings greater than $\zeta_s/\mu = 2$. This is somewhat beyond the range in Figure 3 which is most applicable to marine structures and cable systems. Other approaches using random vibration analysis have been taken by Kennedy and Vandiver (35) and by Whitney, Chung and Yu (45). Kennedy and Vandiver's model was developed solely for the cable strumming problem; limited results have been achieved. Whitney, Chung and Yu developed a general random vibration model for predicting lateral vibration displacements and accelerations due to vortex shedding; extensive calculations were made for the problem of analyzing the motions of long, flexible ocean mining pipes.

The coefficients for a cubic fit to the data for the excitation force coefficient $C_{LE}$ in Figure 6 have been computed and are based upon all of the data points shown there. This cubic equation is given by

$$C_{LE} = a_1 + b_1 Y_{EFF,MAX} + c_1 Y^2_{EFF,MAX} + d_1 Y^3_{EFF,MAX}. \tag{14}$$

These new coefficients are listed as $a_1$, $b_1$, $c_1$ and $d_1$ in Table 5. This fitted curve to the data is considered to be valid between $Y_{EFF,MAX} = 0$ and $Y_{EFF,MAX} = 1.25$ ($2Y_{EFF,MAX} = 2.5$). The results in the table can be employed as inputs to a predictive model for the strumming oscillations of a flexible cable. For a flexible cable or structure the average value of $C_{LE}$ over a given length $L$ is (2,5)

$$C_{LE} = \frac{\int_0^L C_{LE}(z)\,\psi_i(z)\,dz}{\int_0^L \psi_i(z)\,dz} \tag{15}$$

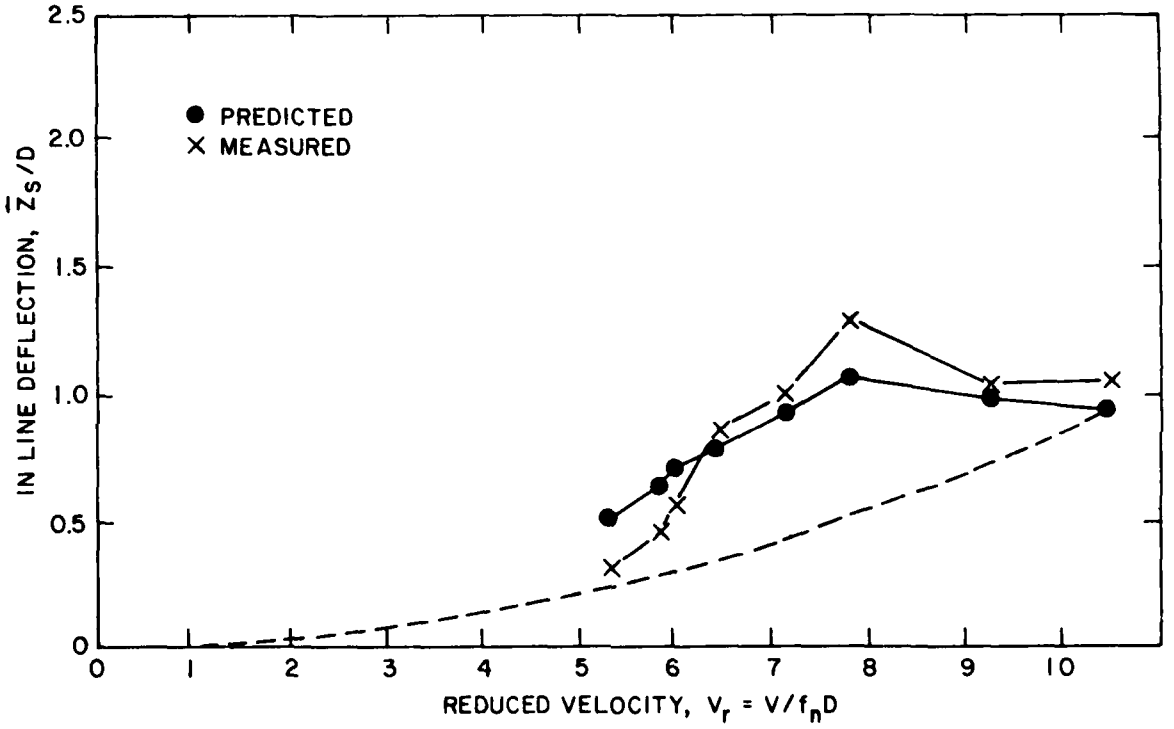


Fig. 26 — The predicted steady tip deflection $Z_s$ of an oscillating flexible cantilever compared to the measured values (relative density $SG = 3.5$) shown in Fig. 7; from Every, King and Griffin (26). The prediction using a constant $C_D = 1.2$ is shown as a dashed line.

Table 5
Excitation Force Coefficient $C_{LE}$, equation (14);
data from Fig. 6

Force coefficient: $C_{LE} = a_1 + b_1 Y_{EFF,MAX} + c_1 Y^2_{EFF,MAX} + d_1 Y^3_{EFF,MAX}$
where $a_1 = 0.12$, $b_1 = 2.12$, $c_1 = -3.57$, $d_1 = 1.45$
and the standard deviation of the curve $\sigma = 0.1$.

Effective displacement: $Y_{EFF,MAX} = \dfrac{(\bar{Y}_{MAX}/D)}{\gamma_i}$ , $\gamma_i = \dfrac{|\psi_i(z)|_{MAX}}{I_i^2}$

In terms of $\bar{Y}_{MAX}/D$,

$$C_{LE}|_{\bar{Y}_{MAX}} = a_1 + (b_1/\gamma_i)(\bar{Y}_{MAX}/D) + (c_1/\gamma_i^2)(\bar{Y}_{MAX}/D)^2 + (d_1/\gamma_i^3)(\bar{Y}_{MAX}/D)^3$$

where the factor $\gamma_i$ is evaluated for a given set of end fixities, i.e. free-pinned, pinned-pinned, clamped-clamped, etc. Hence $\bar{Y}_{MAX}/D$ is the *peak* displacement along the beam. The factor $\gamma_i$ can be calculated from the data listed in references 2 and 5.

It is important to note that the coefficient $C_{LE}$ represents only the excitation force on the structure or cable. For vibrations in water it is necessary to have an accurate and precise representation of the coefficients of the added mass, hydrodynamic damping and hydrodynamic inertia forces. These coefficients are not as well characterized as $C_{LE}$, but they can be derived from the total force measurements of Sarpkaya (14), for example, as shown in Figures 5 and 6.

Several handbooks and catalogues of relevant data are available to augment the results contained in this report. These include a survey of steady drag coefficients for cables subjected to cross flow currents (50) and a detailed handbook of hydrodynamic coefficients for moored array components (51). The report by Dalton (50) is a compilation of steady drag coefficients for stranded steel and synthetic fiber cables. These data are tabulated according to the source and in each case a critical assessment is made concerning the reliability of the experimental fingings. The report by Pattison, Rispin and Tsai (51) is a lengthy and detailed compilation of hydrodynamic force coefficients for moored array components of various shapes (cylinders, spheres, spheriods, streamlined bodies, etc.) and for cables and cable fairings. The authors also make an assessment of the quality and quantity of the experimental data that they include in their report. Solutions to a number of example problems are given in order to illustrate the application of the data.

## 5. COMPUTER CODES FOR CABLE STRUMMING ANALYSIS

As the state of the ocean engineering art steadily progresses, more and more stringent demands are being placed upon the performance of cable structures and moorings. In particular, displacement tolerances and constraints in response to currents are ever tightening; fatigue is becoming an important design consideration; and the sensitivity of acoustic sensors has increased to the point that they cannot differentiate between legitimate acoustic targets and slight variations in their vertical position. All of these are problems that are aggravated by cable strumming.

In order for an engineer to be able to design a structure or cable system to meet the constraints imposed by operational and environmental requirements, he must be able to assess the effect of strumming on the structure in question. Numerical techniques to predict strumming have been developed using the models described in this report and a related report (2) as well as other models which account for the effect of strumming on cable structures. For the most part, the strumming and structural analysis models are separate; however, a few codes have integrated the two types of analyses. The earliest codes that accounted for strumming were static models that allowed the user to specify drag coefficients; other codes performed the strumming analysis and supplied the drag coefficients. Recently, the capability to do strumming calculations continuously has been incorporated into a dynamic model. This allows strumming effects to be modeled and updated virtually continuously as a cable system changes geometry.

### 5.1 NATFREQ, a Strumming Prediction Computer Code

NATFREQ was developed by the Naval Civil Engineering Laboratory (NCEL) for calculating natural frequencies, mode shapes, and drag amplification factors for taut cables with attached masses. Drag amplification factors calculated by NATFREQ using the Skop-Griffin strumming model (16,23) are used as inputs to the DESADE and DECEL1 structural analysis models. The solution technique is based on a new, efficient iterative algorithm (52). The computed results have been compared to simple laboratory experiments with good agreement. One of the cases analyzed using the algorithm was a 4700

m (15,400 ft) cable with 380 attached bodies. The calculated mode shape for mode number 162 is shown in Figure 27. This mode is excited by current velocities near one knot and thus is likely to occur in practice. The complexity of the response is evident.

An accurate prediction of the strumming-induced drag amplification depends upon accurate knowledge of the natural frequencies and mode shapes of the cables in their higher modes. When the cable system has large numbers of attached masses, the prediction of the cable modes and frequencies must be done numerically. NATFREQ is ideally suited to this type of analysis. NATFREQ presently is being compared with the results from the 1981 Castine Bay cable strumming experiments described in Section 3.

### 5.2 Cable Structure Static Analysis Computer Codes

*5.2.1 The DESADE Code.* DESADE was developed by NRL for computing the current-induced static deflections of cable structures (39). The solution technique is the method of imaginary reactions. This is a powerful method that usually converges rapidly; however, it has been shown to be sensitive to problems where the cable tension is low and/or the current velocity is high. DESADE can accommodate a complex cable structure with multiple interconnections and a variety of cable materials. An option exists to perform parametric studies to determine the effect of structural changes or various current regimes on the deformation response. Strumming of the cables can be handled by specifying increased drag coefficients obtained from other models.

A simplified approach to the drag amplification routine in DESADE has been described for application to mooring system design (53). The code also has been employed recently in a design study (54) of the riser power cable segment that provides the link between a floating OTEC power plant and the bottom-resting cable segment that transmits electric power to shore. The required input to the program is listed in detail in reference 39, and the code is available to interested users from NRL or NCEL.

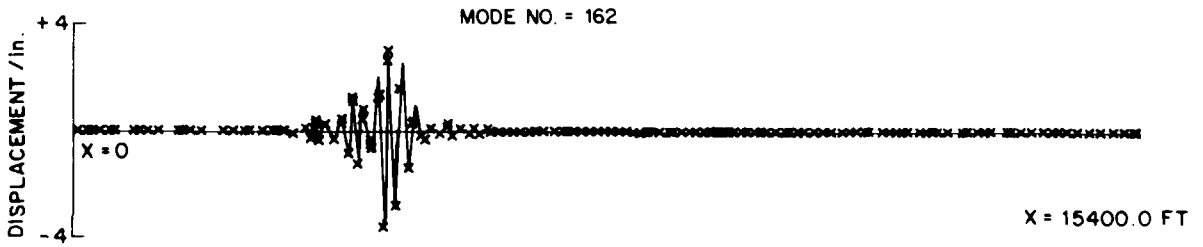


Fig. 27 — The calculated mode shape for a 4700 m (15400 ft) long marine cable with 380 attached sensor housings; from Sergev and Iwan (52)

The importance of including increased drag due to strumming was made apparent in a comparison between the DESADE model and data from an at-sea cable structure experiment and by the results of the 1981 Castine experiments. The at-sea test was of the SEACON II structure; it is discussed in reference 38 and in Section 3.3 of this report.

The cables comprising the delta module of the SEACON array had uniform currents incident over their lengths and were found to be subject to cable strumming. As shown in Section 4.3, the strumming vibrations lead to increases in the effective steady drag coefficients. Since the steady drag coefficient is a basic parameter in all array motion computations, an accurate knowledge of its value is required in order to validate the various models for the analysis of cable structures.

The calculated steady drag coefficient was frequently 150 to 230% greater than the value of the nominal stationary-cable drag coefficient $C_{DO}$ because of strumming of the SEACON II array. Large increases in the resulting drag loads would be expected to have a significant effect on the magnitude of the predicted array motions. The delta cables of the SEACON II array did not undergo a pure mode, resonant lock-on response to the strumming forces. However, the strumming-amplified drag coefficients measured during well-controlled laboratory experiments that were characterized by resonant lock-on have been validated for applications in practice by the SEACON II computations and measured array motions. A similar validation of the strumming-amplified drag coefficients is given by Every, King and Griffin for the case of a model cantilever beam in a steady current (26).

*5.2.2 Variations of DESADE.* NCEL has made modifications to its version of DESADE resulting in the re-named program DECEL1. The modifications include: user conveniences; plotting of structure shape and current field; iteration limits to prevent unexpected high execution costs; and three dimensional current field specification using data from up to four current meter strings. A new users manual (55) has been prepared that includes experience gained from using the program.

### 5.3 SEADYN, a Dynamic Analysis Model

SEADYN is a nonlinear finite-element cable system model being developed by NCEL. Both the static and dynamic behavior of cable systems can be simulated. A wide variety of situations can be modeled, including: pay-out and reel-in, time varying current fields, point loads and surface excitations.

The Skop-Griffin strumming model (16,23) has been incorporated into SEADYN. Strumming calculations are updated in a dynamic simulation whenever the relative velocity of the cable through the water changes by 10%. This is an arbitrary interval and can be changed by the user. To date, the strumming calculation option has been used infrequently because of the disparity between the relatively small number of nodes required for adequate hydrodynamic modeling as compared to the large number required to obtain an adequate description of mode shape for the strumming model. Modeling with a large number of nodes results in a large cost penalty in computing the gross response of the cable. A more efficient, fast algorithm such as the one used in NATFREQ could be adapted to perform cost effective strumming calculations. SEADYN has a default, Reynolds number-dependent drag coefficient built in, but this can be over-ridden if the user specifies a drag coefficient or function based on other independent knowledge or calculations. Further information concerning SEADYN is available from NCEL.

### 5.4 The SLAK Code

A finite element code for predicting the natural frequencies and mode shapes of slack cables was developed from a previously existing code as part of a recent Navy cable dynamics research program (2). A finite element formulation is employed and the range of validity is not limited to small sag-to-span ratios, ($s/l < 0.12$) as are most existing linear theories. The code is also valid for arbitrary locations of the end points (an inclined cable), it is three-dimensional, and it permits concentrated applied loads (attached discrete masses) at various locations along the cable. The principal results that are obtained from the code in its present form are the (in-air) natural frequencies, the support reaction forces, the equilibrium shape of the cable, and the natural mode shapes with respect to the equilibrium

shape. The code is called SLAK and it is discussed in further detail in reference 2 of this report. Further information concerning SLAK is available from NRL.

### 5.5 Other Applicable Computer Codes

DESADE is one of two existing cable structure models that explicitly takes account of strumming-induced hydrodynamic force amplifications of marine cables. However, other codes to predict vortex-excited oscillations are being developed because of the importance of vortex shedding-related problems in marine applications. VORTOS is a computer code developed by Atkins Research and Development in the the United Kingdom. The essential features of the code are described in a recently published report (56). This program predicts the dynamic response of a flexible cylinder to vortex-excited oscillations in steady flow. The vibration amplitude and frequency response in a steady flow may be calculated for flexible cylindrical members of a variety of marine structures. The calculation is based upon experimental measurements of the cross flow response and the excitation forces using spring-mounted rigid cylinders and flexible cylinders (8).

The program is based upon the reasonable assumption that the lift force at each position along the length of a cylinder in steady flow is a sinusoidal function of time and is dependent upon the local incident flow velocity and the displacement amplitude. This point is discussed in Section 2 of this report. The structure is represented by simple finite elements (at this stage up to eleven in number) and the appropriate mass and stiffness matrices. The vortex shedding frequency is determined from the reduced velocity $V_r$ for each element and is assumed to lock-on close to the natural frequency of the structure at the critical velocities described in Sections 2, 3 and 4 of this report. More specifically, lock-on is assumed to occur if the Strouhal frequency $f_s$ is between 0.8 $f_n$ and 1.6 $f_n$ (56). The resonant, vortex-excited lift forces are derived as a function of displacement amplitude for each vibrating element from experimental data. An iterative procedure is employed to calculate the steady-state deflected shape of the cylindrical member and the maximum bending stress is determined from the curvature.

A flexible cylinder of diameter $D = 25$ mm (1 in.) was employed to give an example of the results that were obtainable with VORTOS. The cylinder behaved very much like a cable since it had an aspect ratio of $L/D = 240$ and a low value of structural damping. The important features of the code are described in more detail in reference 56, which also includes a worked example problem with output and a listing of the input data required to exercise the code.

A computer code, MARISE, for the analysis of marine riser dynamics has been developed by the Shell Development Company. A variation of this code recently was modified to accommodate a wake-oscillator type of vortex shedding analysis (57). Predictions have been made of the oscillatory behavior of Cognac platform piles in various configurations during lowering and driving operations (19,24). Fair agreement was obtained between the MARISE predictions and model test results.

The computer code UCIN-CABLE has been developed to analyze the dynamics of underwater cables (58). This program models a flexible cable by a series of rigid cylinders connected end-to-end by ball and socket joints. The size, shape and mass of each of the segments is arbitrary. Spherical attached masses and anchors can be included in the cable system at various locations. It also is possible to include fluid effects on the cable such as normal and tangential fluid drag forces, added mass and buoyancy (59). No vortex shedding effects are included explicitly, but the normal drag coefficient presumably can be specified to account for strumming-induced drag amplification effects.

The dynamic analysis of the cable model is a specialization of a recently-developed analysis technique for general chain systems. The cable is assumed to be perfectly flexible, the dimensions and physical parameters of each segment are arbitrary, and the externally-applied forces on each section also are arbitrary. The UCIN-CABLE code is expected by its developers to be effective in studying the nonlinear, three-dimensional dynamic behavior of long cables. A user's manual is available (58).

These numerical models represent the first generation of cable strumming analyses. As more experience is gained using these models, other ideas and techniques for improving the state of the art

of calculating the effects of marine cable strumming undoubtedly will evolve. At this time these models represent the most up-to-date understanding of strumming effects.

## 6. CABLE STRUMMING SUPPRESSION

Oscillations due to vortex shedding can be suppressed or reduced in amplitude by altering the mass (natural frequency) and damping of the structure or by attaching some device to alter the flow field and thereby to reduce the coherence of the vortex shedding. It is usually costly and time consuming to modify the structure in order to change its damping and natural frequency. Most marine cables are lightly damped and increasing the damping usually is not attempted, but sometimes the natural frequency can be changed sufficiently by increasing the tension in the cable. The suppression of strumming oscillations is a complex problem because the slenderness (length/diameter) of most practical cable array segments is very large and many cable vibration modes often participate in the oscillations, as shown earlier in this report. The mooring and anchoring cables for an OTEC plant will have extremely large ratios of length/diameter, will have nonuniform currents incident upon them, and often will be inclined to the flow. These factors complicate the suppression of strumming oscillations as compared to the suppression of oscillations for a cylindrical beam or other flexible member.

The strumming oscillations of cables are usually reduced by attaching some form of external device to interfere with the vortex shedding sufficiently to reduce the oscillations to tolerable levels. Most strumming suppression devices increase the hydrodynamic damping and, possibly, the cable's added mass and the effective frontal area of the cable that is projected into the flow. The steady hydrodynamic drag force then is increased relative to the drag on a stationary cable.

Several studies have been conducted in recent years to categorize the various types of strumming suppression devices and to attempt to understand more completely the mechanics of strumming suppression. A paper by Every, King, and Weaver (60) discusses the vortex excited vibrations of cables and cylinders and compares the effectiveness of various devices which have been developed to suppress the oscillations. Hafen and Meggitt (61) have consolidated the existing data on most available

devices that have been used to suppress strumming oscillations. They suggest criteria for making comparisons among different strumming suppression devices. Vandiver and Pham (62) reported the findings from field tests of four different types of strumming suppression devices. The devices tested included different types and configurations of synthetic fiber helical fringe and "haired" windings of various lengths and linear spacings. Three of the devices completely suppressed the oscillations but they resulted in a substantial drag penalty. Water tunnel flow visualization experiments showed that the devices did not eliminate vortex shedding but tended to reduce the spanwise coherence of the vortices.

Kline, Nelligan and Diggs (63) also have studied and have attempted to categorize various devices that have been developed to suppress cable strumming. Meggitt, Kline and Pattison (64) have conducted a series of experiments in one of the DTNSRDC towing channels to provide a data baseline for characterizing the behavior of representative strumming suppression devices in a quantitative manner. Several bare cables of various constructions (Kevlar, steel, nylon) and several cables with attached devices (helical fringe, helical ridge, segmented airfoil) were tested using the towing fixture shown in Figure 14. A neutrally buoyant segmented foil reduced the strumming amplitude to negligible levels and also substantially reduced the drag on the cable. Both the helical fringe and helical wrap reduced the cable strumming to tolerable levels, but the helical fringe increased the steady drag coefficient by a factor of 100 percent. Strumming of the bare cables resulted in typical steady drag coefficients between $C_D$ = 1.7 and 2.9 (64).

It is typical of much of the cable strumming suppression literature that considerable scatter is evident in the existing data and that conflicting results often appear. There is little agreement between laboratory and at-sea data. Many devices for cable strumming suppression are Reynolds number dependent in terms of their operating characteristics, and data often are given for a particular device at a Reynolds number different from an intended application. However, the trends that have been found are now discussed in terms of potential OTEC mooring cable applications.

Hafen and Meggitt (61) generally have classified the most effective strumming suppression devices into four categories. These include helical ridges (strakes), flexible ribbon fairings, "fringe" fairings

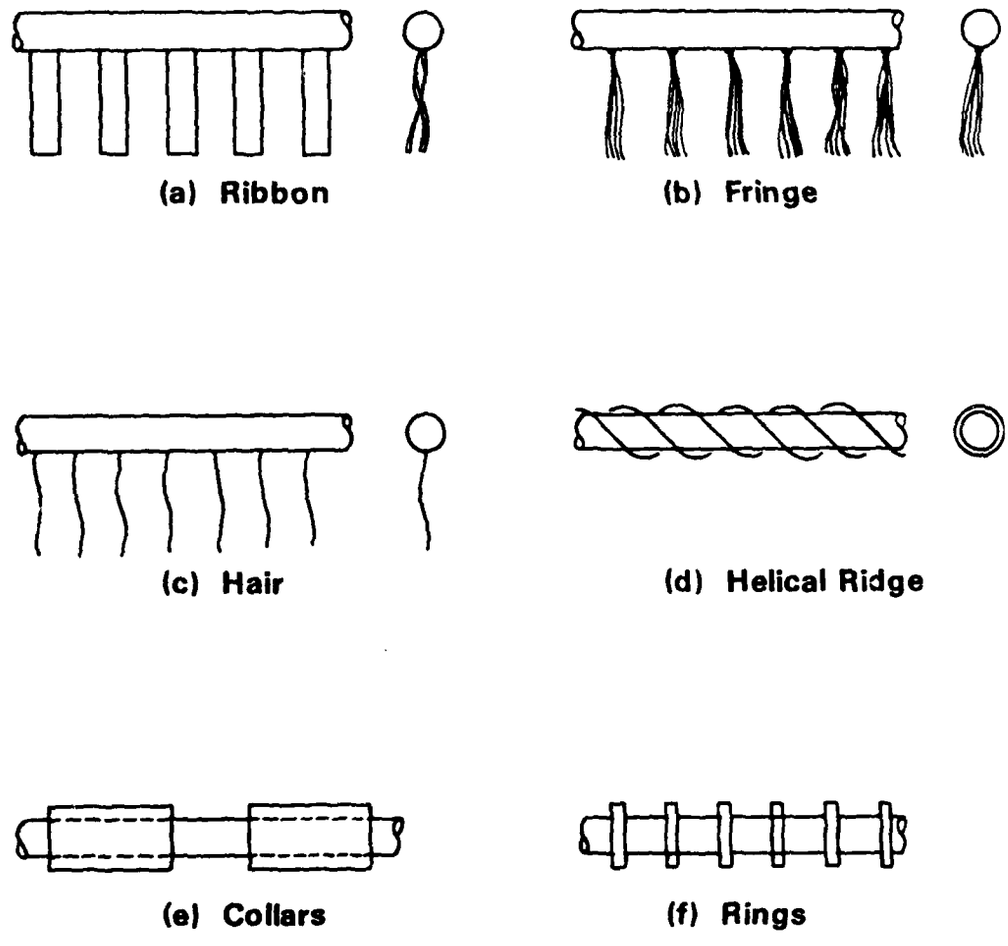


Fig. 28 — A line drawing of several common cable strumming suppression devices; from Every, King and Weaver (60)

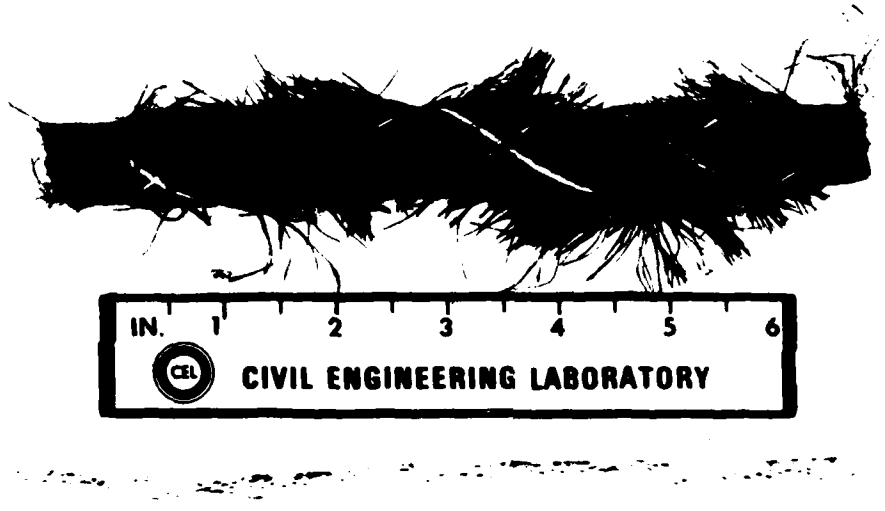


Fig. 29 — Examples of Philadelphia Resin Corporation haired fairings. Top: brush fairings applied helically on a 19.2 mm (0.75 in.) diameter cable. Bottom: cotton fuzz applied helically on a 6.4 mm (0.25 in.) diameter Kevlar cable. Photograph from Hafen and Meggitt (61).

and "haired" fairings. Rigid, streamlined airfoil-shaped devices also are used effectively to suppress strumming under some circumstances (60, 64). These devices yield relatively low drag coefficients but they are expensive, difficult to handle and can undergo large lateral deflections (kiting) at nonzero angles of attack. Specially designed cable handling equipment is required. Rings and sleeves have been tried but generally these devices have proven to be ineffective as strumming suppressors. The various devices are sketched in Figure 28, from Every, King and Weaver (60). Photographs of two typical "haired fairing" devices studied by Hafen and Meggitt (61) are shown in Figure 29.

With the exception of the airfoil-shaped suppression device, virtually all other strumming suppression devices tend to produce large increases in the steady hydrodynamic drag, as shown by Meggitt, Kline and Pattison (64). The hydrodynamic drag on a helical fringe fairing was as high as $C_D = 4.8$ on a 12.7 mm (0.5 in) Kevlar cable with a 76 mm (3 in) fringe over its entire length (64). The same cable with four helical wraps over its length had a $C_D = 2.5$. Other measured values of the drag ranged from $C_D = 0.72$ (ballasted airfoil) to $C_D = 2.9$ (helical fringe 25.4 mm (1 in) long over the entire cable). Typically the same bare cable underwent sustained strumming vibrations and $C_D = 2.3$. Thus a drag penalty is paid in most applications and an optimum design for a strumming suppression device must weigh the relative importance of reduced vibration levels against the penalty of increased drag. The drag penalty is an important consideration in the design of deep water cable arrays such as the ocean-based OTEC plant mooring system in 1200 m (3900 ft) to 1800 m (5900 ft) depths.

## 7. OTEC MOORING CABLE APPLICATIONS

The marine industry is now developing the capability to deploy mooring systems at 600 m (2000 ft) to 1500 m (5000 ft) depths. Long-term production technology has not been developed for application to these water depths although relatively short-term drilling has been conducted at depths to 1200 m (4000 ft). A recent OTEC mooring system technology development plan (1) has identified several promising mooring configurations for OTEC plants at 1200 m (3900 ft) to 1800 m (5900 ft) depths. These are shown in Figure 30. Two independent studies were conducted (65, 66) to compare the various mooring systems. The proposed concepts were evaluated on the bases of economics, hardware

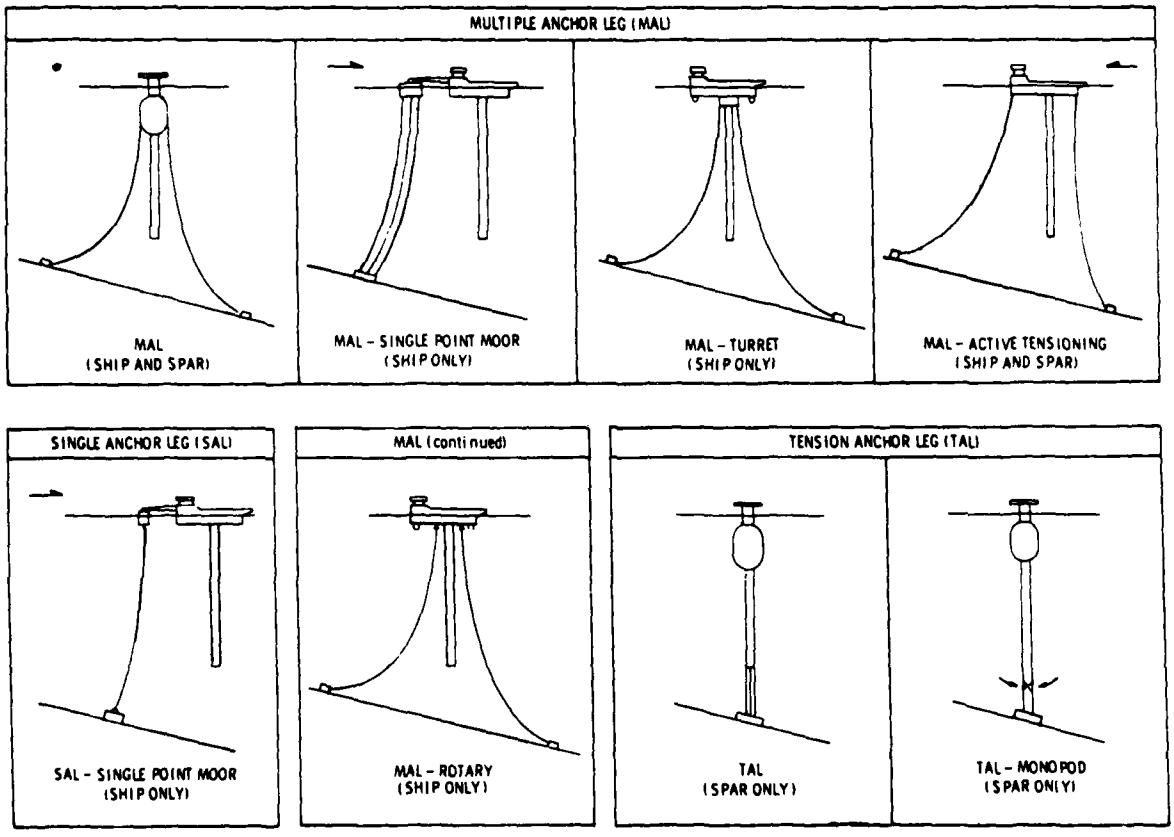


Fig. 30 — Examples of OTEC power plant mooring configurations from recent conceptual design studies (1)

availability, development required, and various risk parameters. One study, conducted by Lockheed Ocean System (65), selected a tension anchor leg system for the spar OTEC plant and an eight-leg multiple anchor leg system for the barge-mounted plant. A study conducted by M. Rosenblatt and Son (66) resulted in the choice of an eight-leg multiple anchor system for the spar plant and a twelve-leg system for the barge.

A subsequent review (67) of these two studies stressed the importance of detailed assessments of the corrosion, abrasion, and fatigue characteristics of the OTEC mooring system components. It also was noted that a multiple anchor leg mooring system is feasible for a 10/40 MW OTEC pilot plant in the 1986 time frame. However, such a system cannot be designed using off-the-shelf components and a feasible design will depend upon a number of technical innovations. The review concluded that a tension anchor leg mooring system was not feasible for an OTEC plant in the configuration that was proposed.

A fatigue analysis of a moored cable structure deployed in these water depths can be conducted using the analysis techniques that are described in this report and in related reports (2, 5, 6, 26). The importance of a detailed analysis of fatigue, corrosion, and abrasion effects during the marine cable system design process also has been emphasized by Berteaux (68).

The OTEC cold water pipe design report by Griffin (5) contains a number of step-by-step examples of how to conduct an analysis of cylindrical structure's susceptibility to vortex-excited fatigue effects. Though the examples directly concern the cold water pipe, it is straightforward to apply the step-by-step procedures to a cable strumming analysis. These worked examples and their relation to the various steps in a cable strumming analysis are summarized in Table 6. Likewise, the recent report by Griffin, Ramberg, Skop, Meggitt and Sergev (2) deals with the analysis of cable strumming problems. Factors such as the choice of cable damping and added mass coefficients, slack cable effects, and unsteady and steady hydrodynamic loads are discussed. The applicable results from the latter report are summarized in Table 7 for easy reference.

Table 6
Analysis of OTEC Mooring Cable Strumming Problems;
Corresponding Example Problems from Reference 5.*

| Problem | Example Problem/Page (Reference 5) |
|---|---|
| Cable strumming displacement amplitudes and cable reduced damping. | Example 4.1 Calculation of the effective cross flow displacement amplitude and reduced damping; page 15. |
| | Example 5.1 Calculation of the vortex-excited cross flow displacement amplitude; page 41. |
| Cable strumming steady drag amplification. | Example 5.2 Calculation of the steady drag amplification $C_D/C_{D0}$ due to cross flow vortex-excited oscillations; page 43. |
| Critical incident flow velocities for the onset of cable strumming. | Example 8.1 Calculation of the critical incident flow velocities when the natural periods/frequencies are known; page 55. |
| | Example 8.3 Calculation of the critical velocities and natural periods; page 62. |
| Effective and/or virtual mass of a marine cable. | Example 3.2 Calculation of the reduced damping parameter (and the effective mass ratio); page 11. |
| | Example 8.2 Calculation of the effective mass ratio $m_e/\rho D^2$; page 57. |

*"OTEC Cold Water Pipe Design for Problems Caused by Vortex-Excited Oscillations," Naval Research Laboratory (NRL) Memorandum Report 4157, March 1980.

Table 7
Analysis of OTEC Mooring Cable Strumming Problems;
Corresponding Sections from Reference 2.*

| Problem | Chapter or Appendix/Page (Reference 2) |
|---|---|
| Dynamics of Taut Marine Cables. | Appendix A; page 119. |
| Dynamics of Slack Cables; Criteria for the Onset of Slack Cable Effects. | Appendix B; page 123. |
| Marine Cable Added Mass and Damping Coefficients. | Appendix C; page 140. |
| Cable Strumming Prediction Models. | Appendixes D and E; pages 153 and 161. |
| Effects of Vortex Shedding Coherence Length, Surface Roughness, Velocity Shear and Turbulence, Reynolds Numbers, Cable Yaw or Inclination. | Chapter 2, Sections 2.3 to 2.7; pages 14 to 51. |

*"The Strumming Vibrations of Marine Cables: State of the Art," Naval Civil Engineering Laboratory (NCEL) Technical Note No. N-1608, May 1981.

The complete body of example problems and engineering data in these reports provides a basis for the cable system designer to conduct a step-by-step analysis of the mooring and anchoring cable systems for an ocean-sited OTEC power plant.

## 8. SUMMARY

### 8.1 Findings and Conclusions

Problems associated with the shedding of vortices often have been overlooked or crudely approached on an ad hoc basis until the recent past in relation to the design of marine structures and cable systems, largely because reliable experimental data and design procedures have not been available. However, the dynamic analysis of marine structures and cable systems has become increasingly important and sophisticated in order to accurately predict stress distributions and operational lifetimes in the ocean environment. The strumming vibrations of marine cables have serious consequences because they take place at relatively high frequencies and are a potential cause of fatigue for system components. They also are a cause of increased hydrodynamic drag and steady deflections. Strumming can introduce acoustic noise in sensor components attached to the cable and can cause abrasion and wear of fittings and of the cables themselves. These vibrations usually are caused by a current flowing past the cable. However, they also are caused sometimes by low-frequency wave drift forces and long period swells when the cable extends downward from the vicinity of the ocean surface.

This report has summarized the present state-of-the-art concerning the strumming vibrations of marine cables, as related to the analysis and design of OTEC mooring and anchoring cable systems. Reliable data now are in hand for the dynamic response of and hydrodynamic forces on model-scale [illegible] and cables, and based upon these findings empirical and semi-empirical prediction models [illegible] developed and calibrated for use in practice. Many of the recent findings have come from [illegible] dynamics research program, the results obtained from that program through [illegible] Civil Engineering Laboratory report (2).

Detailed information now is available for the resonant vortex-excited response of model cylindrical structures and cables that are characterized by subcritical Reynolds numbers, i.e., $Re < 2(10^5)$. There also is reasonably detailed knowledge of the steady drag amplification that accompanies vortex-excited oscillations. This force amplification causes increased steady deflections of the structure or cable and practical design methods have been developed to predict this steady deflection, as shown in this report and others (6, 26). Unsteady hydrodynamic strumming force coefficients have been measured at moderate Reynolds numbers, $Re = 10^3$ to $10^4$, and these coefficients have been employed in the development of the practical design procedures that are described here and in several related reports and paper (2, 4, 5, 6, 26). Virtually all of the measurements of cylinder and cable dynamic responses and forces have been made in the subcritical Reynolds number range that is most applicable to cable strumming problems.

### 8.2 Recommendations

Though reasonable engineering approximations must be made, the design procedures and the experimental data base that are summarized in this and related reports are recommended for use in cable system design practice. Procedures are described for predicting a particular system's susceptibility to vortex-excited strumming oscillations. In addition, a reasonable data base from steady and dynamic response and force coefficient measurements also is provided to aid in detailed calculations of the system response, if that approach is necessary. A number of computer codes also are available to assist the designer and some have been calibrated against both field measurements and laboratory-scale test data. The analysis of the data from recent field tests presently is underway, but additional well-controlled field tests are needed to broaden the existing data base.

## 9. REFERENCES

1. S. Bailey and L. Vega, "OTEC Mooring and Anchoring Systems: Technology Development Plan," Eighth Ocean Energy Conference Proceedings, Marine Technology Society: Washington, D.C, in press, 1982.

2. O.M. Griffin, R.A. Skop, S.E. Ramberg, D.J. Meggitt and S.S. Sergev, "The Strumming Vibrations of Marine Cables: State of the Art," Naval Civil Engineering Laboratory Technical Note No. N-1608, May 1981.

3. T. Sarpkaya, "Vortex-Induced Oscillations, A Selective Review," Trans. ASME, Series E, J. Applied Mechanics, Vol. 46, 241-258, 1979.

4. R. King, "A Review of Vortex Shedding Research and Its Application," Ocean Engineering, Vol. 4, 141-171, 1977.

5. O.M. Griffin, "OTEC Cold Water Pipe Design for Problems Caused by Vortex-Excited Oscillations," NRL Memorandum Report 4157 (March 1980); see also Ocean Engineering, Vol. 8, 129-209, 1981.

6. O.M. Griffin, "Steady Hydrodynamic Loads Due to Vortex Shedding from the OTEC Cold Water Pipes," NRL Memorandum Report 4698, January 1982.

7. O.M. Griffin and G.H. Koopmann, "The Vortex-Excited Lift and Reaction Forces on Resonantly Vibrating Cylinders," J. Sound and Vib., Vol. 54, 435-448, 1977.

8. R.B. Dean, R.W. Milligan and L.R. Wootton, "An Experimental Study of Flow-Induced Vibration," E.E.C. Report 4, Atkins Research and Development, Epsom (U.K.), 1977.

9. D.T. Tsahalis and W.T. Jones, "Vortex-Induced Vibrations of a Flexible Cylinder Near a Plane Boundary," Offshore Technology Paper OTC 3991, May 1981.

10. I.G. Currie, R.T. Hartlen and W.W. Martin, "The Response of Circular Cylinders to Vortex Shedding," *Flow-Induced Structural Vibrations:* symposium, Karlsruhe (Germany) August 14-16, 1972, E. Naudascher (ed.), Springer: Berlin, 1974.

11. G. Buresti and A. Lanciotti, "Vortex Shedding From Smooth and Rough Circular Cylinders Near a Plane Boundary," Aeronautical Quarterly, Vol. 28, 305-321, February 1979.

12. M.G. Hallam, N.J. Heaf and L.R. Wootton, "Dynamics of Marine Structures," Construction Industry Research and Information Association (CIRIA) Report UR 8, London, 1978.

13. R.B. Dean and L.R. Wootton, "An Analysis of Vortex Shedding Problems in Offshore Engineering," Atkins Research and Development Report No. 77/14, Epsom (UK), 1977.

14. T. Sarpkaya, "Transverse Oscillation of a Circular Cylinder in Uniform Flow," Proc. ASCE, J. Waterways, Port, Coastal and Ocean Div., Vol. 104, 275-290, 1978.

15. O.M. Griffin, "Vortex-Excited Cross Flow Vibrations of a Single Cylindrical Tube," Trans. ASME, Series J. Pressure Vessel Tech., Vol. 102, 158-166, 1980; see also *Flow-Induced Vibrations,* S.S. Chen and M.D. Bernstein (eds.), ASME: New York, 1-10, 1979.

16. R.A. Skop and O.M. Griffin, "On a Theory for the Vortex-Excited Oscillations of Flexible Cylindrical Structures," J. Sound and Vib., Vol. 41, 263-274, 1975; see also "The Vortex-Induced Oscillations of Structures," J. Sound and Vib., Vol. 44, 303-305, 1976.

17. W.D. Iwan, "The Vortex-Induced Oscillation of Elastic Structural Elements," Trans. ASME, Series B, J. Engrg. Indus., Vol. 97, 1378-1382, 1975.

18. R. King, M.J. Prosser and D.J. Johns, "On vortex excitation of model piles in water," J. Sound and Vib., Vol. 29, 169-188, 1973.

19. R. King, "Model Tests of Vortex Induced Motion of Cable Suspended and Cantilevered Piles for the Cognac Platform," BHRA Report RR 1453, January 1978.

20. O.M. Griffin, "A universal Strouhal number for the "locking-on" of vortex shedding to the vibrations of bluff bodies," J. Fluid Mech., Vol. 85, 591-606, 1978.

21. S.S. Chen, "Crossflow-Induced Vibrations of Heat Exchanger Tube Banks," Nuc. Engrg. and Design, Vol. 47, 67-86, 1978.

22. O.M. Griffin and S.E. Ramberg, "On vortex strength and drag in bluff body wakes," J. Fluid Mech., Vol. 69, 721-728, 1975.

23. R.A. Skop, O.M. Griffin and S.E. Ramberg, "Strumming Predictions for the Seacon II Experimental Mooring," Offshore Technology Conference Preprint OTC 2884, 1977.

24. F.J. Fischer, W.T. Jones and R. King, "Current-Induced Oscillations of Cognac Piles During Installation—Prediction and Measurement," in Proc. Symp. on Practical Experiences with Flow-Induced Vibrations (Preprints), Karlsruhe, Vol. I, 216-228, September 1979.

25. G. Grimminger, "The Effect of Rigid Guide Vanes on the Vibration and Drag of a Towed Circular Cylinder," David Taylor Model Basin Report 504, April 1945.

26. M.J. Every, R. King and O.M. Griffin, "Hydrodynamic Loads on Flexible Marine Structures Due to Vortex Shedding," ASME Paper 81—WA/FE—24, November 1981.

27. O.M. Griffin, J.H. Pattison, R.A. Skop, S.E. Ramberg and D.J. Meggitt, "Vortex-Excited Vibrations of Marine Cables," Proc. ASCE, J. Waterway, Port, Coastal and Ocean Div., Vol. 106, No. WW2, 183-204, 1980.

28. J. Dale, H. Menzel and J. McCandless, "Dynamic Characteristics of Underwater Cables: Flow Induced Transverse Vibrations," Naval Air Development Center Report NADC-AE-6620, 1966.

29. J.R. Dale, "Water Drag Effects of Flow Induced Cable Vibrations," Naval Air Development Center Report NADC-AE-6731, 1967.

30. J.H. Pattison, "Measurement Technique to Obtain Strumming Characteristics of Model Mooring Cables in Uniform Currents," David Taylor Naval Ship Research and Development Center Report SPD 766-01, April 1977.

31. J.H. Pattison, "Measurement Technique to Obtain Strumming Characteristics of Model Mooring Cables in Uniform Currents; Data Supplement," Supplement to Report SPD 776-01, DTNSRDC, April 1977.

32. J.E. Kline, E. Fitzgerald, C. Taylor and T. Brzoska, "The Dynamic Response of a Moored Hydrophone Housing Assembly Subjected to a Steady Uniform Flow," MAR Inc., Technical Report No. 237, February 1980.

33. J.K. Vandiver, "A Field Study of Vortex-Excited Vibrations of Marine Cables," Offshore Technology Conference Preprint 2491 (May 1976).

34. J.K. Vandiver and T.P. Pham, "Performance Evaluation of Various Strumming Suppression Devises," MIT Ocean Engineering Department Report 77-2, March 1977.

35. M. Kennedy and J.K. Vandiver, "A Random Vibration Model for Cable Strumming Prediction," Proceedings of CIVIL ENGINEERING IN THE OCEANS IV, ASCE: New York, 273-292, 1979.

36. J.K. Vandiver, private communication, October 1981.

37. E.J. Softley, J.F. Dilley and D.A. Rogers, "An Experiment to Correlate Strumming and Fishbite Events on Deep Ocean Moorings," GE Document 77SDR 2181, General Electric Co.: Re-Entry and Environmental Systems Division, 1977.

38. T.R. Kretschmer, G.A. Edgerton and N.D. Albertsen, "Seafloor Construction Experiment, SEA-CON II; An Instrumented Tri-Moor for Evaluating Undersea Cable Structure Technology," Civil Engineering Laboratory Technical Report R-848, December 1976.

39. R.A. Skop and J. Mark, "A Fortran IV Program for Computing the Static Deflections of Structural Cable Arrays," Naval Research Laboratory Report 7640, August 1973.

40. M.B. Kennedy, "A Linear Random Vibration Model for Cable Strumming," Ph.D. Thesis, Massachusetts Institute of Technology, May 1979.

41. C.M. Alexander, "The Complex Vibrations and Implied Drag of a Long Oceanographic Wire in Cross-Flow," Ocean Engineering, Vol. 8, 379-406, 1981.

42. R.D. Blevins, *Flow-Induced Vibration,* Van Nostrand-Reinhold: New York, 1977.

43. R.T. Hartlen and I.G. Currie, "Lift-Oscillator Model of Vortex-Induced Vibrations," Proceedings of the ASCE, Journal of Engineering Mechanics, Vol. 96, 577-591, 1970.

44. R.D. Blevins and T.E. Burton, "Fluid Forces Induced by Vortex Shedding," Trans. ASME, Series I, J. Fluids Engrg., Vol. 98, 19-24, 1976.

45. A.K. Whitney, J.S. Chung and B.K. Yu, "Vibrations of Long Marine Pipes Due to Vortex Shedding," Trans. ASME., J. Energy Resources Technology, Vol. 103, 231-236, September 1981.

46. T. Sarpkaya and R.A. Shoaff, "Numerical Modeling of Vortex-Induced Oscillations," CIVIL ENGINEERING IN THE OCEANS IV, ASCE: New York, 504-517, 1979.

47. S.E. Hurlbut, M.L. Spaulding and F.M. White, "Numerical Solution of the Time Dependent Navier-Stokes Equations in the Presence of an Oscillating Cylinder," in *Numerical Solution of Non-steady Flows,* ASME: New York, 201-206, 1978.

48. O.M. Griffin, R.A. Skop and S.E. Ramberg, "Resonant, Vortex-Excited Vibrations of Structures and Cable Systems," Offshore Technology Conference Preprint OTC 2319, 1975.

49. "Wind and Water-Current-Induced Oscillations in Tubulars," Petroleum Engineer International, Vol. 51, No. 12, 46-62, October 1979.

50. W.L. Dalton, "A Survey of Available Data on the Normal Drag Coefficient of Cables Subjected to Cross Flow," *Civil Engineering Laboratory Report* CR 78.001, Port Hueneme, CA, August 1977.

51. J.H. Pattison, P.P. Rispin and N.T. Tsai, "Handbook on Hydrodynamic Characteristics of Moored Array Components," David Taylor Naval Ship Research and Development Center Report SPD-745-01, March 1977.

52. S. Sergev and W.D. Iwan, "The Natural Frequencies and Mode Shapes of Cables with Attached Masses," Navy Civil Engineering Laboratory Technical Memorandum M-44-79-3, April 1979.

53. R.A. Skop and F. Rosenthal, "Some New Approximation Techniques for Mooring System Design," Marine Technology Society Journal, Vol. 13, No. 6, 9-13, 1979.

54. R.A. Lindman, J.C. Oliver, W.L. Jawish and P.L. Steiner, "OTEC Riser Cable Loads Analysis and Ocean Engineering Design Criteria," Giannotti and Associates Report No. 79-045-005, May 1980 (Preliminary Report).

55. S. Sergev, "DECEL 1 Users Manual — A Fortran IV Program for Computing the Static Deflections of Structural Cable Arrays," Civil Engineering Laboratory, Technical Note N-1584, August 1980.

56. W.A. Evers and R.B. Dean, "VORTOS—A Program for the Calculation of Vortex-Induced Oscillations in Steady Flow," Atkins Research and Development Report 1978/APR/2, Epsom (V.K.), April 1978.

57. R.P. Nordgren, "Dynamic Analysis of Marine Risers with Vortex Excitation," 37th Petroleum Mechanical Engineering Workshop and Conference Proceedings, ASME: New York, 33-40, September 1981.

58. J.W. Kamman and R.L. Huston, "Users Manual for UCIN-CABLE: Underwater Cables," Report on ONR Contract N00014-76C-0139, University of Cincinnati, 1981.

59. R.L. Huston and J.W. Kamman, "A Representation of Fluid Forces in Finite Segment Cable Models," *Computers and Structures*, Vol. 14, 281-287, 1981.

60. M.J. Every, R. King and D.S. Weaver, "Vortex Excited Vibrations of Cylinders and Cables and Their Suppression," Ocean Engineering, Vol. 9, in press, 1982.

61. B.E. Hafen and D.J. Meggitt, "Cable Strumming Suppression," Naval Civil Engineering Laboratory Technical Note n-1499, September 1977.

62. J.K. Vandiver and T.Q. Pham, "Performance Evaluation of Various Strumming Suppression Devices," MIT Ocean Engineering Department Report 77-2, March 1977.

63. J.E. Kline, J.J. Nelligan and J.S. Diggs, "A Survery of Recent Investigations into the Nature of Cable Strumming, its Mechanism and Suppression," MAR Inc. Technical Report 210, July 1978.

64. D. Meggitt, J. Kline and J. Pattison, "Suppression of Mooring Cable Strumming" Proceedings of the Eighth Ocean Energy Conference, Paper IB5, Marine Technology Society: Washington, DC, in press, 1982.

65. Lockheed Missiles and Space Company, "Preliminary Designs for OTEC Stationkeeping Subsystems (SKSS); Summary Report, February 1980.

66. M. Rosenblatt and Son, Inc., "Modular OTEC Platform SKSS Designs," February 1980.

67. Det norske Veritas, "OTEC Stationkeeping Subsystems (SKSS) Design Criteria," September 1980.

68. H.O. Berteaux, *Buoy Engineering*, Wiley-Interscience: New York, 1976.

*U.S. GOVERNMENT PRINTING OFFICE: 1982 361-334/511 1-3


DATE
FILMED
7-8